5-2018

Neogene Stratigraphy and Paleoenvironments in the Lauca Basin of Northern Chile

Amanda Jones
University of Nebraska-Lincoln, acjones9393@hotmail.com

NEOGENE STRATIGRAPHY AND PALEOENVIRONMENTS IN THE LAUCA BASIN OF NORTHERN CHILE

by

Amanda Jones

A THESIS

Presented to the Faculty of

The Graduate College at the University of Nebraska

In Partial Fulfillment of Requirements

For the Degree of Master of Science

Major: Earth and Atmospheric Sciences

Under the Supervision of

Professor Sherilyn Fritz

Lincoln, Nebraska

May, 2018

NEOGENE STRATIGRAPHY AND PALEOENVIRONMENTS IN THE LAUCA BASIN OF NORTHERN CHILE

Amanda Jones, M.S.

University of Nebraska, 2018

Advisor: Sherilyn Fritz

This thesis examines a late Miocene to Pliocene sedimentary succession in the Lauca Basin, a topographically isolated, fluvio-lacustrine basin in the northern Chilean Altiplano. A sedimentary section within the Lauca Basin, composed of Lauca Formation sediments, was investigated using stratigraphic and petrographic analyses to define the Miocene to Pliocene paleoenvironmental history of the region. Geochronologic results indicate the section ranges in age from approximately 5.57 +/- 0.20 Ma to 5.44 +/- 0.16 Ma. The sedimentology of 36 samples was described, and twelve samples were analyzed petrographically. Five lithofacies were characterized: laminated mudstone (Fl), volcaniclastic mudstone (Fv), carbonate (C), evaporite (E), and muddy sandstone (SF). These lithofacies were used to characterize sedimentary structures and interpret depositional environments. These ranged from deposition from suspension in a moderate to deep lacustrine environment (Fl and Fv); deposition and precipitation of carbonates and evaporites in closed, possibly ephemeral environment (C and E); and deposition in a shallow high-energy lacustrine environment (SF). The dominant presence of evaporites and the dominantly laminated sedimentary units throughout the section suggest a closed lacustrine environment, and are indicative of seasonal or periodic changes in sediment supply. The evolution of the sedimentary section is inferred from the depositional environments combined with prior studies of the Miocene-Pliocene transition to produce

a regional history at higher temporal resolution. The evolution of the Lauca Basin was influenced strongly by evaporation and precipitation, with significantly lesser influences of volcanism, tectonism, and sedimentary supply. The bulk of sediments deposited in the sedimentary section were from an arid, saline, occasionally ephemeral lacustrine environment.

ACKNOWLEDGEMENTS

My achievements and the completion of my thesis project would not have been possible without the assistance provided by my advisor, Dr. Sherilyn Fritz of the University of Nebraska-Lincoln. She provided me the opportunity to pursue a Master's degree in a non-traditional setting as well as a much needed source of advice. Another invaluable element to this project was one of my committee members, Dr. Matt Joeckel, whom I would like to thank for his extensive assistance on the sedimentological and petrographic analyses components of this project. I would also like to thank the University of Nebraska-Lincoln and the Department of Earth and Atmospheric Sciences for the use of their facilities and resources, my fellow graduate students Melina Feitl and Justin Ahren, Paul Baker and Wout Salenbien of Duke University, my committee member Dr. Richard Kettler, Dr. Chris Fielding and Dr. Tracy Frank for use of their research laboratory when taking photomicrographs. Many of my goals for this project would not have been possible without the assistance and immense knowledge of my support system.

Finally, I would like to thank my family and friends for their support and encouragement. My motivation to follow through and seek a degree beyond my undergraduate degree is due to you, and you all constantly inspire me to improve.

TABLE OF CONTENTS

LIST OF FIGURES

LIST OF TABLES

CHAPTER 1: INTRODUCTION

The Lauca Basin (Fig. 1), which lies at the western margin of the northern Chilean Altiplano, is a topographically isolated fluvio-lacustrine basin, consisting of two subbasins: a main southern subbasin and a shallow northern subbasin. Altitudes within the basin average 4100 m, and drainage trends eastward to the Coipasa Basin in Bolivia. The basin has an active felsic stratovolcanic margin to the east and a dormant and heavily eroded felsic stratovolcanic margin to the west. Tephra from these volcanoes are used as stratigraphic markers that can be dated using a variety of geochronological methods to generate a regional chronology for the basin fill. The horizontal stratification of the youngest basin sediment fill demonstrates limited tectonic displacement since ~6 Ma. Because of this limited tectonic displacement, the basin's sedimentary record has a great potential for paleoenvironmental reconstruction (Kott et al., 1995).

The paleoenvironmental record of the Lauca Basin is of particular importance for five reasons: 1) established tephra geochronology; 2) persistent hydrographic and geographic boundaries since the late Miocene; 3) arid climate and limited chemical weathering; 4) Miocene to Pliocene sedimentary record; and 5) most westerly position among all of the Andean basins (Gaupp et al., 1999). These factors make a study of the stratigraphic section significant for developing a comprehensive regional record of the Miocene-Pliocene transition. Kott et al. (1995) and Gaupp et al. (1999) previously evaluated the paleoenvironmental and geological history of the Lauca Basin. These studies were broad in geographic extent and focused on the large-scale Mio-Pliocene history of the basin. In contrast, this thesis analyzes a single outcrop in detail to produce a

regional history at higher temporal resolution, incorporating a detrital zircon geochronology measured on bounding tuffaceous samples.

CHAPTER 2: SETTING

2.1. Global

Multiple parameters influence climate on a global scale, including changes in Earth's geography and topography, atmospheric composition, and orbital forcing. These parameters affected climate in the Neogene, as significant changes in continental and oceanic topography, geography, and greenhouse gas concentrations took place. The Neogene is characterized by long-term global cooling and drying, commencing in the Paleogene and culminating in extensive Northern Hemisphere glaciations at the start of the Pleistocene, at roughly 2.6 Ma (Zachos et al., 2001). Multiple proxy records suggest that El Nino Southern Oscillation (ENSO)-like variability was present during the mid to late Miocene and early Pliocene, most likely affecting the late middle Miocene climatic optimum and the subsequent cooling (Brierley et al., 2010; Fedorov et al., 2010; Galeotti et al., 2010; Batenburg et al., 2011). Despite overall global cooling through the Miocene and Pliocene, the early Pliocene was a moderately warm period, with global temperatures approximately 3°C warmer than present (Wara et al., 2005).

Neogene uplift of major mountain chains (including the Himalayas, Alps, Pyrenees, and Andes) has been hypothesized to both directly and indirectly influence the changes in climate that followed, as well as affect erosion rates and associated isostatic changes (Hay et al., 2002). One of the most significant tectonic events of the Neogene was the connection of North and South America at the Isthmus of Panama, which took

place sometime between the mid-Miocene (15 Ma) and late Pliocene (3 Ma). The exact timing of closure has been recently debated, and emerging sources suggest these events may have taken place earlier (in the Miocene) than was previously accepted (Montes et al., 2015; O'Dea et al., 2016). This connection and closure of the seaway between North and South America, whenever it occurred, likely led to extensive changes in ocean circulation and climate (Haug et al., 1998). By the mid-Pliocene, many of the global oceanic gateways and continental positions were similar to present times, meaning that many geologic and climatic analyses of this time period can be used to better understand the processes occurring presently.

2.2. Regional

The uplift of the Central Andes during the mid-Miocene initiated a regional transition in western portions of the continent from semi-aridity to hyper-aridity due to orographic effects and global climate cooling during the period (Rech et al., 2006). Regionally, uplift created a rain-shadow, effectively blocking moisture from the South American summer monsoon from reaching the Atacama region to the west (Rech et al., 2006) and producing endorheic systems from the late Paleocene through the Pliocene (Mortimer, 1980; Díaz et al., 1999). This climate transition generated a series of dry saline lacustrine basins (salars) on the Chilean Altiplano (Díaz et al., 1999; Gaupp et al., 1999; de Wet et al., 2015).

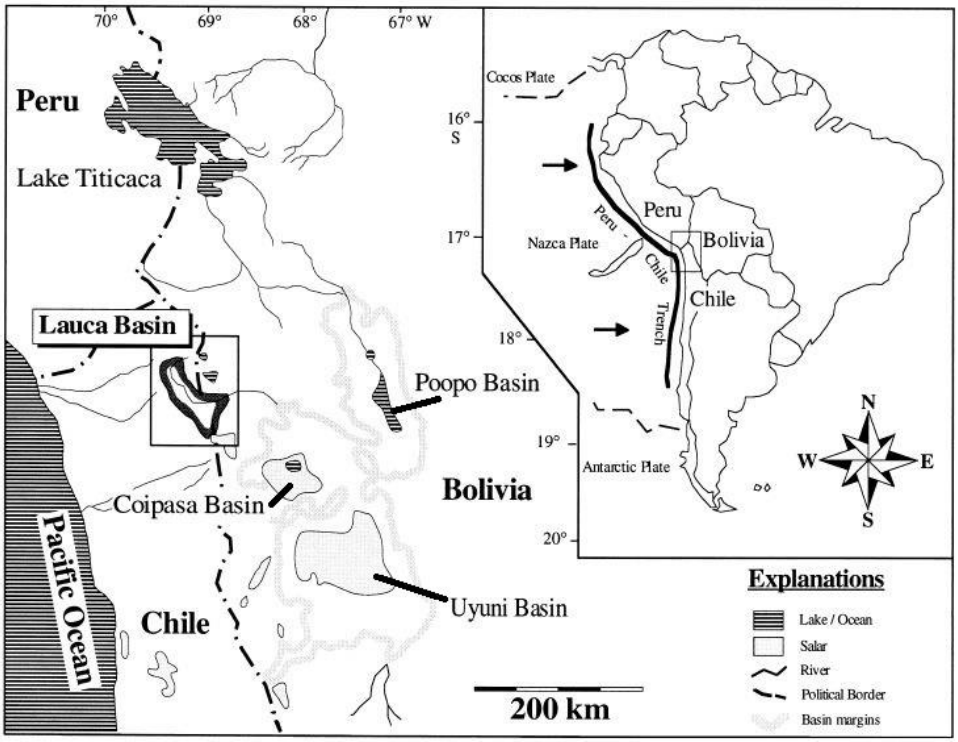

Fig. 1: Map showing a) the location of the Lauca Basin within South America (box), and b) its location relative to other regional basins (outlined in gray). Reprinted from Gaupp et al., 1997.

Fig. 2: View of a representative sedimentary sequence in the Lauca Basin, looking northeast toward the active volcanic arc (Guallatire) in the distance.

The Lauca Basin (18.3500˚S, 69.3000˚W) lies within the westernmost sub-basin of the northern Chilean Altiplano (also referred to as the Andean Plateau or Bolivian Plateau), which lies mostly in Bolivia and Peru, barely extending westward into Chile (Fig. 1). Deposits within the basin trend NW-SE and are bordered by eastern active volcanoes (Fig. 2) and western dormant and heavily eroded Miocene-age volcanoes (Gaupp et al., 1999). Sediment comprises Miocene and Pliocene aged clastic, carbonate, and evaporitic deposits. Volcanic sediments comprise dominantly dacitic and rhyolitic ash and volcaniclastic fragments from the bordering felsic volcanic margins (Worner et al., 1988; Gaupp et al., 1999). The majority of sediment fill is designated as the Lauca Formation; a lacustrine formation that is 120 meters thick with a basal age of approximately 6.4 Ma. It uncomformably overlies the Quebrada Macusa Formation (approximately 11 Ma) and is overlain by the Lauca ignimbrite (2.3 ± 0.7 Ma) (Charrier et al., 2004; Garcia et al., 2011). The oldest deposits in the Lauca Formation are present in the main southern sub-basin (Kott et al., 1995). Previous studies in the basin have defined it as a fluvio-lacustrine environment under arid to semi-arid conditions (Kott et al., 1995; Gaupp et al., 1999).

Gaupp et al. (1999) proposed four main units for the Lauca Basin fill: 1) Stage 1 (>6.4 Ma, or late Miocene) – alluvial and fluvial red beds and paleosols, with vascular-plant root traces; subordinate intervals of lacustrine deposition with diatomites; 2) Stage 2 (6.4-3.7 Ma, or late Miocene to early Pliocene) – shallow ephemeral lakes or playas, with evidence of minor evaporite deposition, episodic sheet floods, debris flows, and tuff beds preserved; 3) Stage 3 (3.7-2.6 Ma, or late Pliocene) – braidplain containing small, open lakes; and 4) Stage 4 (2.7-<0.25 Ma, or latest Pliocene to Pleistocene) – glacial

sedimentation and erosion, fluvial deposition, and small open lakes. Thus, the depositional environments within the basin are chiefly alluvial or fluvial and lacustrine. Lacustrine facies are dominant in the central basin and thin towards the margins. The sequence studied in this thesis falls approximately within Stage 2 of Gaupp et al.'s (1999) environmental stage summary for the Lauca Basin.

CHAPTER 3: METHODS

3.1. Field Methods

A 31-meter sedimentary succession within the Lauca Formation was sampled on the southern shore of the Rio Lauca (18.5792583˚S, 69.1609861˚W, 4057 masl) by Dr. Sherilyn Fritz and Dr. Paul Baker in November 2014 (Fig. 3). Representative samples of lithofacies determined in the field were collected, and sample elevations were measured with a hand-held level. Thirty-six lithological samples were retrieved from the outcrop itself, along with five ancillary samples from nearby locations.

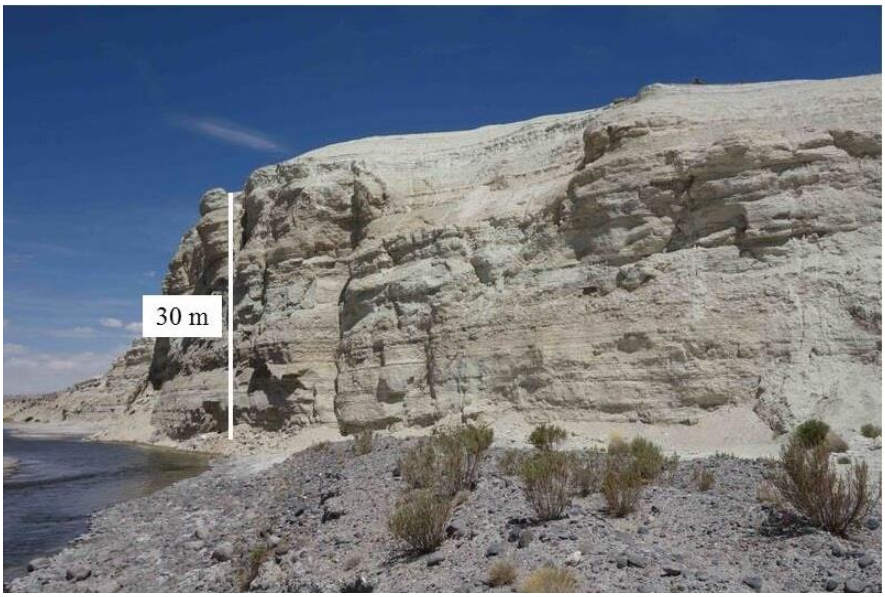

Fig. 3: Outcrop along the shore of the Rio Lauca in the Lauca Basin, Chile (18.5792583˚S, 69.1609861˚W). Outcrop faces north and is approximately 31 m in height.

3.2. Laboratory Methods

The hand samples collected in the field were systematically described in the laboratory, and a stratigraphic column was generated using the CorelDraw Graphics Suite. Sample descriptions included color in wet and dry conditions using the Munsell Soil Color Chart (Munsell Color, 2010), reaction with 10% hydrochloric acid, and descriptions of sedimentary lithology and sedimentary features. Terminology used in the latter descriptions are based on Stow (2005) and include terms used to describe stratal thicknesses, stratal geometries, relevant structure characteristics (erosional structures, depositional structures, post-depositional deformation and dewatering structures, biogenic sedimentary structures, and chemogenic sedimentary structures), and facies designations.

Twelve of the 41 lithologic hand samples were selected for thin-section petrography on the basis of their lithologic characteristics in hand specimen. Collectively, they are considered representative of the range of lithofacies described in this study. These samples are, in ascending stratigraphic order: LB20, LB21, LB4, LB18, LB13, LB11, LB26, LB30, LB31, LB34, LB35, and LB40 (Appendix B). Petrographic thin sections were produced by Spectrum Petrographics (Vancouver, WA).

Prior to thin-sectioning, hand samples were marked in order to designate the preferred cut line and to label the top of the sample, which would subsequently be labeled on the thin section slide. Each sample was labeled with its corresponding sample number and wrapped in foil. Thin sections were vacuum impregnated with a clear epoxy resin and mounted on a standard two inch by three inch (roughly 50 mm by 76 mm) glass slide with a standard 30 μm thickness, permanently mounted cover glass, and orientation

markings indicating the “top” of the hand sample.

Thin-section observations were systematic and included assessments of sediment texture and lithology, sediment grains, authigenic minerals, sedimentary fabric, biogenic structures, organic material, and subsequent category non-conforming notes. Terminology used in lithofacies descriptions follow Bullock (1985), which describes a range of features visible in petrographic analysis and contains specific definitions for the associated terminology. Characterization of laminae is based on Stow (2006). Analysis of the thin sections was made with an Olympus BH-2 series polarizing light petrographic microscope with a circular rotatable stage and 4X, 10X, and 40X magnification power scope objectives.

Thin sections were photographed to capture the unique characteristics of each slide, using a Nikon Eclipse E400 POL microscope, and scanned using a Prior OptiScanII Stage with an attached Nikon Eclipse Ci.

The stratigraphic and petrographic descriptions are used to define facies and depositional environments in the sedimentary succession. A logical letter coding system is used to better define and express the characteristics of each lithofacies and microfacies (Table 1). The letter coding system used was generated based on multiple precedent studies (e.g., Smith, 1980).

Table 1: Facies and structure letter codes.

Siliciclastic Codes		Organochemical Codes	
S	Sandstone	C	Carbonate
SF	Muddy Sandstone	E	Evaporite
F	Fines (claystone, siltstone, mudstone)		
Sedimentary Structure Codes			
b	Brecciation		
c	Calcareous, minor carbonate		
e	Minor evaporite		
f	Fossiliferous		
g	Graded lamination		
i	Interbedded, interlaminated		
l	Laminated		
m	Massive (structureless)		
n	Inverse graded lamination		
o	Ooids		
p	Peloids		
v	Volcaniclastic (tephra)		

Ages for samples near the base and top of the outcrop (LB5 and LB36) were established by collaborators through detrital zircon geochronology on volcanic tuffs. Measurements were made at the Arizona LaserChronCenter of the University of Arizona by laser ablation–multicollector–inductively coupled plasma–mass spectrometry (LA-MC-ICP-MS) following established procedures (Gehrels, 2014). These data are compared to and integrated with earlier ages derived from K/Ar geochronology (Kott et al., 1995; Gaupp et al., 1999; Wörner et al., 2000).

CHAPTER 4: RESULTS

4.1. Stratigraphy

Sediments in this succession are composed of laminated and volcaniclastic mudstones, carbonate, evaporites, and muddy sandstones (Fig. 4). The lower two meters of the succession are dominantly thin beds of mudstones. The middle fourteen meters

transition to thicker beds of carbonate and evaporite with lenses of mudstones and, more rarely, muddy sandstone. The upper fourteen meters of the succession transition back to dominance of bedded mudstones and lenses of muddy sandstone with much thicker beds than the lower units.

Overall, sedimentary units near the bottom of the succession tend to be much thinner than those in the upper section, with samples LB19-LB13 taking up less than one comprehensive meter. Parallel planar laminae are generally more common throughout the section than wavy, convoluted laminae, especially in mudstones. Ostracodes are the only identifiable fossiliferous features throughout, however, there are a few unidentified fossiliferous features, including possible silicified algal mats. Most of the sediments have a carbonate or evaporite component, and many contain volcaniclastic material. Peloids and ooids are frequent throughout the succession, especially in carbonate and evaporite units.

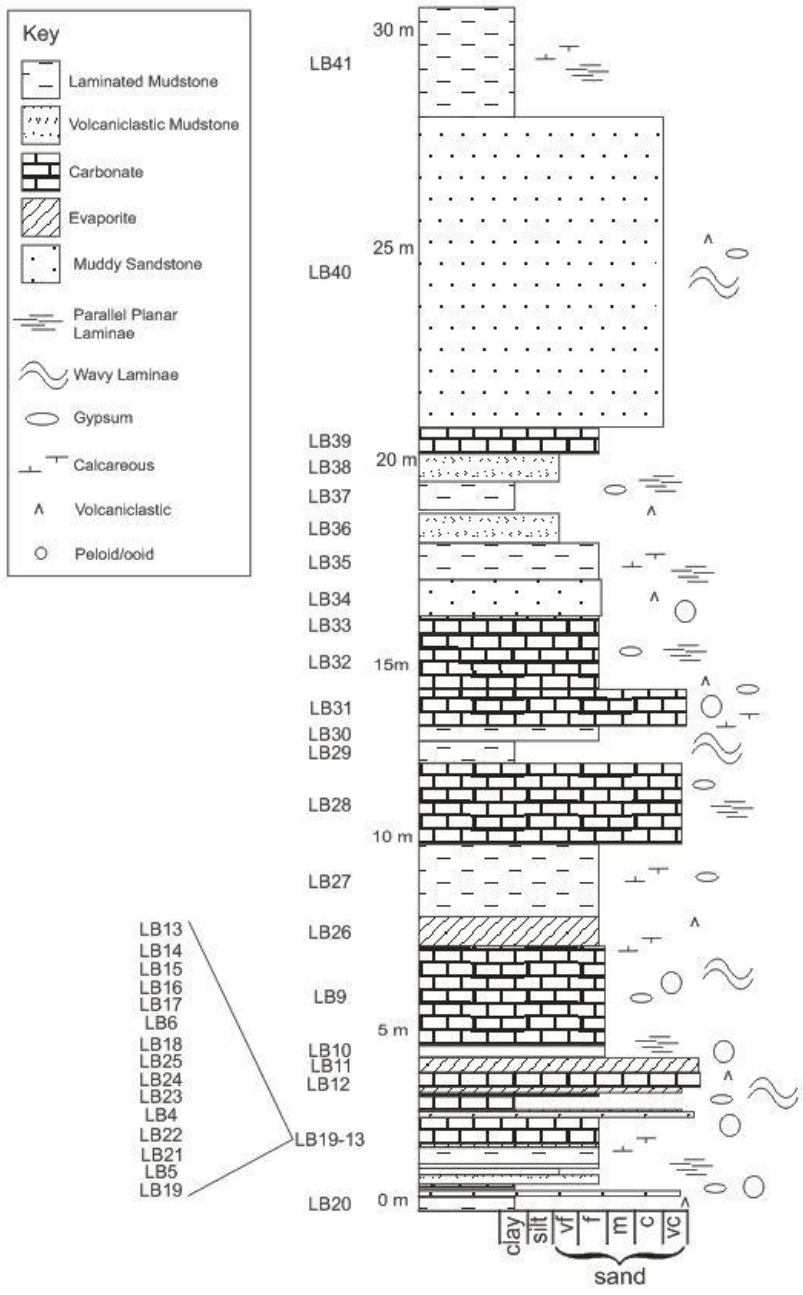

Fig. 4: Stratigraphic column of the 31-meter sedimentary succession (Fig. 3) depicting various rock types and sedimentary features present. Sample numbers are indicated at the left of the stratigraphic column.

4.2. Lithofacies

Five lithofacies (laminated mudstone, volcaniclastic mudstone, carbonate, evaporite, and muddy sandstone) that are representative of distinct depositional

environments are identified (Table 2). These lithofacies are distinguished by sediment type and texture, authigenic minerals, sedimentary fabric and structures, biogenic structures, organic material, and other relevant characteristics. Some of the lithofacies can be subdivided into distinctive microfacies. All lithofacies and microfacies designations are assigned letter codes based on their characteristic features. Thin-sectioned samples are assigned specific microfacies designations, because they were analyzed more comprehensively and microscopically, whereas hand samples are only assigned the broader lithofacies designations. One sample (LB26) was assigned to multiple microfacies within its lithofacies designation, because of varying characteristics and contrasting thin section domains.

Table 2: Lithofacies and microfacies of Lauca Basin outcrop samples. Descriptive letter code designations can be found in Table 1.

Lithofacies	Microfacies	Letter Code	Thin Sections	Hand Samples
Laminated mudstone (Fl)	Non-calcareous	Flp	LB20, LB21	LB19, LB24, LB25, LB10, LB27, LB29, LB37, LB41
	Calcareous	Flcpn	LB30, LB35	
Volcaniclastic mudstone (Fv)	Ashy siltstone	Fv	LB4	LB23, LB36, LB38
	Ashy mudstone	Fv		
	Ashy claystone	Fv		
	Silty ash	Fv		
Carbonate (C)	Sandy carbonate	Cfbp	LB31	LB22, LB6, LB15, LB14, LB12, LB9, LB28, LB32, LB33, LB39
Evaporite (E)	Gypsum and carbonate	EClpon	LB18, LB26	LB16
	Gypsum and clay	EFlcvon	LB13, LB11, LB26	
Muddy sandstone (SF)	Massive	SFmv	LB40	LB5, LB17
	Laminated	SFlv	LB34	

4.2.1. Lithofacies Fl (Laminated Mudstone)

Lithofacies Fl is the most abundant lithofacies in the stratigraphic section and accounts for 12 of the 36 hand samples and 4 of the 12 thin sections. This lithofacies is present throughout the stratigraphic section (Fig. 4). It can be subdivided into two microfacies: non-calcareous (Flp), and calcareous (Flcpn).

The matrix of lithofacies Fl consists of approximately 80% fine-grained clay and 20% silt. There are gradations from nearly pure clay to silty clay in several thin section domains. The clay matrix displays unistrial birefringence, meaning that individual laminae show nearly continuous extinction due to uniformly oriented clay particles settled from suspension. This matrix appears light yellow to yellow in cross-polarized light. Lithofacies Fl varies from non-calcareous to strongly calcareous throughout the section. Few (5-15%) amounts of micritic carbonate are present in a few thin sections. The sediment contains frequent (15-30%) silt and sand grains consisting of plagioclase, oxidized biotite, olivine, and volcanic ash and glassy volcanic rock fragments. Sediment grains are overall subhedral to anhedral, undulating to smooth, and sub-rounded to rounded. Clusters of gypsum crystals that have been partially to fully replaced by chalcedony are common in some thin sections and feature lenticular to sublenticular outlines.

Lithofacies Fl is generally laminated. Individual laminae are discontinuous and irregular, very thin to medium (0.005-4.0 mm thick), and they range from planar parallel to convoluted, wavy, and non-parallel. There are localized very thin to medium (0.05-3.0 mm thick), lenticular laminae. There are very few to few, very thin (0.05-1.0 mm thick) elongate lenses of sand, silt, and carbonate in all thin sections of this lithofacies.

The color of lithofacies Fl is typically greenish gray to light greenish gray (10Y 5/1, 6/1, 7/1, 8/1, 5GY 6/1, 7/1) in hand sample, however, some samples are pale yellow (5Y 7/4, 8/3). Reddish yellow, yellow, and yellowish brown (5Y 8/6, 10YR 7/8, 10YR 5/8) staining and black (10G 2.5/1) mottling is present. The black mottling appears in long and thin undulating lines and dark flecks. The staining (hydrous iron oxides) is present in all thin sections, and, in some places, it is directly associated with weathered biotite grains. This staining appears in long and thick streaks and localized fragments.

Possible current-ripples exist in some thin sections, but they are very faint and poorly preserved. Carbonate peloids and possible filled burrows or elongate lenses appear in this lithofacies, as well as small, black (10G 2.5/1), opaque in cross-polarized light (XPL) and plane polarized light (PPL), fragments that may be organic matter or pyrite fragments. Siliciclastic mud pellets are present in variable numbers and are distinct from clastic grains and carbonate peloids in that there are no concentric markings and the pellets comprise finer and silicate minerals rather than carbonate.

The non-calcareous microfacies (Flp) has only sparse amounts of carbonate throughout the section, excluding carbonate peloids. The calcareous microfacies (Flcpn) displays variable amounts of micritic carbonate overall throughout a given thin section. Micritic carbonate is concentrated more in some areas than in others and is mixed with clay matrix in many sections. This microfacies contains very few ostracodes or silicified algal structures.

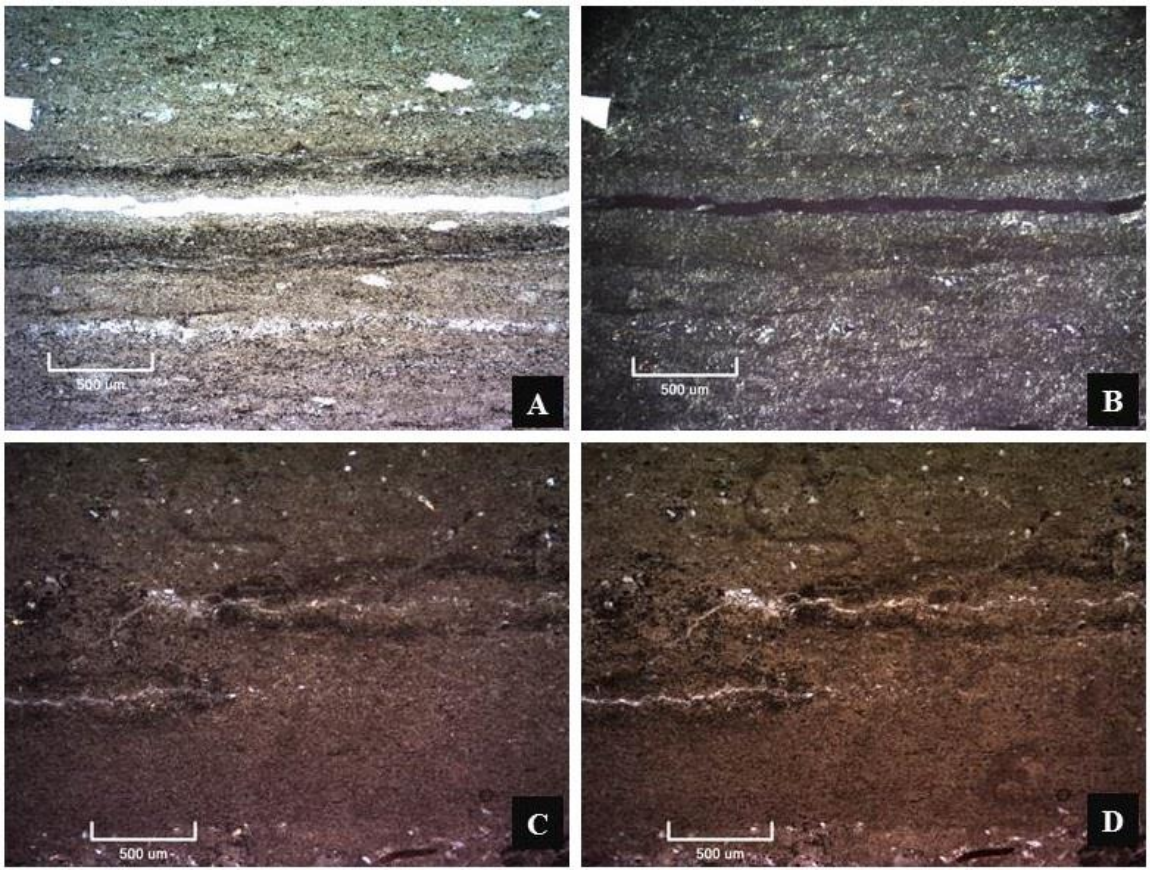

Fig. 5: Photomicrographs of the two distinct microfacies in the mudstone lithofacies (Fl). A) Non-calcareous, polarized light, B) Non-calcareous, cross-polarized light, C) Calcareous, polarized light, D) Calcareous, cross-polarized light. A 500 µm bar is included for scale in the bottom left corner of each photomicrograph.

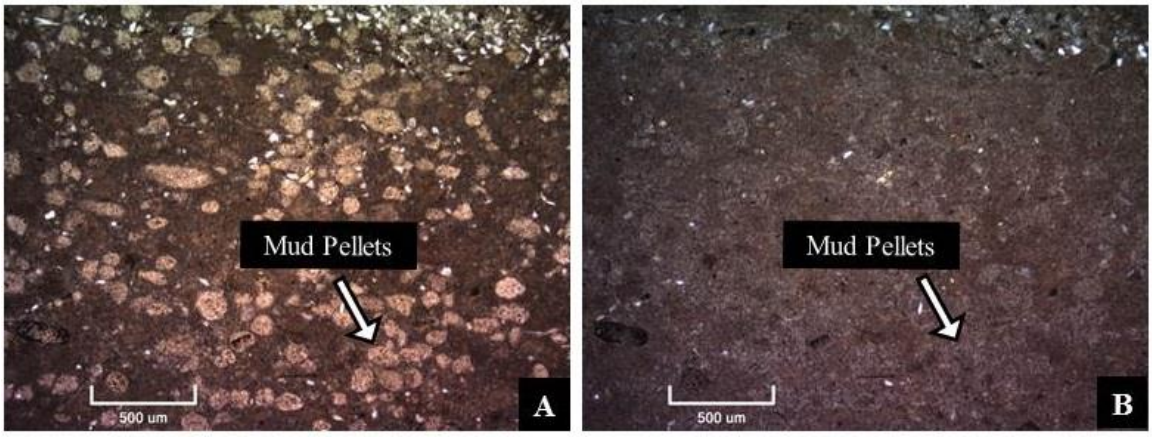

Fig. 6: Photomicrographs of siliciclastic mud pellets from LB35, distinct from other siliciclastic grains present. A) Siliciclastic mud pellets, polarized light, B) Siliciclastic mud pellets, cross-polarized light. A 500 µm bar is included for scale in the bottom left corner of each photomicrograph.

4.2.2. Lithofacies Fv (Volcaniclastic Mudstone)

Lithofacies Fv is one of the two least-abundant lithofacies in the section, accounting for only 4 of the 36 main samples and 1 of the 12 thin sections. This lithofacies exists near the top and bottom of the stratigraphic section (Fig. 4). It can be subdivided into four microfacies: ashy siltstone, ashy mudstone, ashy claystone, and silty ash (all Fv).

The matrix consists of a mixture of very fine-grained clay and silt with very dominant (>70%) glassy volcanic rock fragments and mica. The clay matrix displays unistrial birefringence. This matrix appears light yellow to yellow in cross-polarized light. Sediments in this lithofacies are not calcareous or are only very slightly calcareous. In thin section, dacitic and rhyolitic volcaniclastic fragments from volcanic activity are very dominant (>70%), whereas carbonate and evaporitic material is largely absent. Frequent (15-30%) silt and sand grains are present that consist of plagioclase, oxidized biotite, olivine, and volcanic ash and glassy volcanic rock fragments. Sediment grains are overall subhedral (frequent, 15-30%, euhedral grains are additionally present), undulating to smooth, and subangular. Few (5-15%) volcanic ash fragments appear to have been partially to fully altered to smectitic clays. Very few (<5%) gypsum crystals are present, and those present tend to be acicular and radiating, with lesser amounts of subhedral and lenticular grains.

Laminae are discontinuous and irregular when present; however, massive bedding is generally representative of this lithofacies. Laminae vary in thickness, depending on the thin section domain, but overall tend to be very thin (0.05-0.5 mm thick). Distinct laminae of fine-grained clay, silt, and ash are present.

This lithofacies is typically greenish gray (10Y 5/1, 6/1, 7/1, 8/1) in hand samples, although it is also yellow and pale yellow (5Y 7/3, 8/3, 10YR 6/8, 7/8) in places. Reddish yellow, yellow, and yellowish brown (5Y 8/6, 10YR 7/8, 10YR 5/8) staining is present. The staining (hydrous iron oxides) is, in some places, directly associated with weathered biotite grains. This staining appears in long and thick streaks and localized fragments. Domains with a more dominant volcanic component have more dominant staining.

The ashy siltstone microfacies (Fv) comprises a siliciclastic silt matrix with a dominant (50-70%) volcaniclastic component. The volcanic ash microfacies (Fv) comprises dominant (50-70%) volcanic ash and volcaniclastic sediments. The ashy clay microfacies (Fv) comprises dominant (50-70%) volcanic ash in a clay matrix, with few (5-15%) coarse-grained mineral components. The silty ash microfacies (Fv) comprises dominant (50-70%) volcanic ash in a silty matrix. Feldspar, biotite, and olivine grains are common (30-50%) in both the ashy siltstone (Fv) and silty ash (Fv) microfacies.

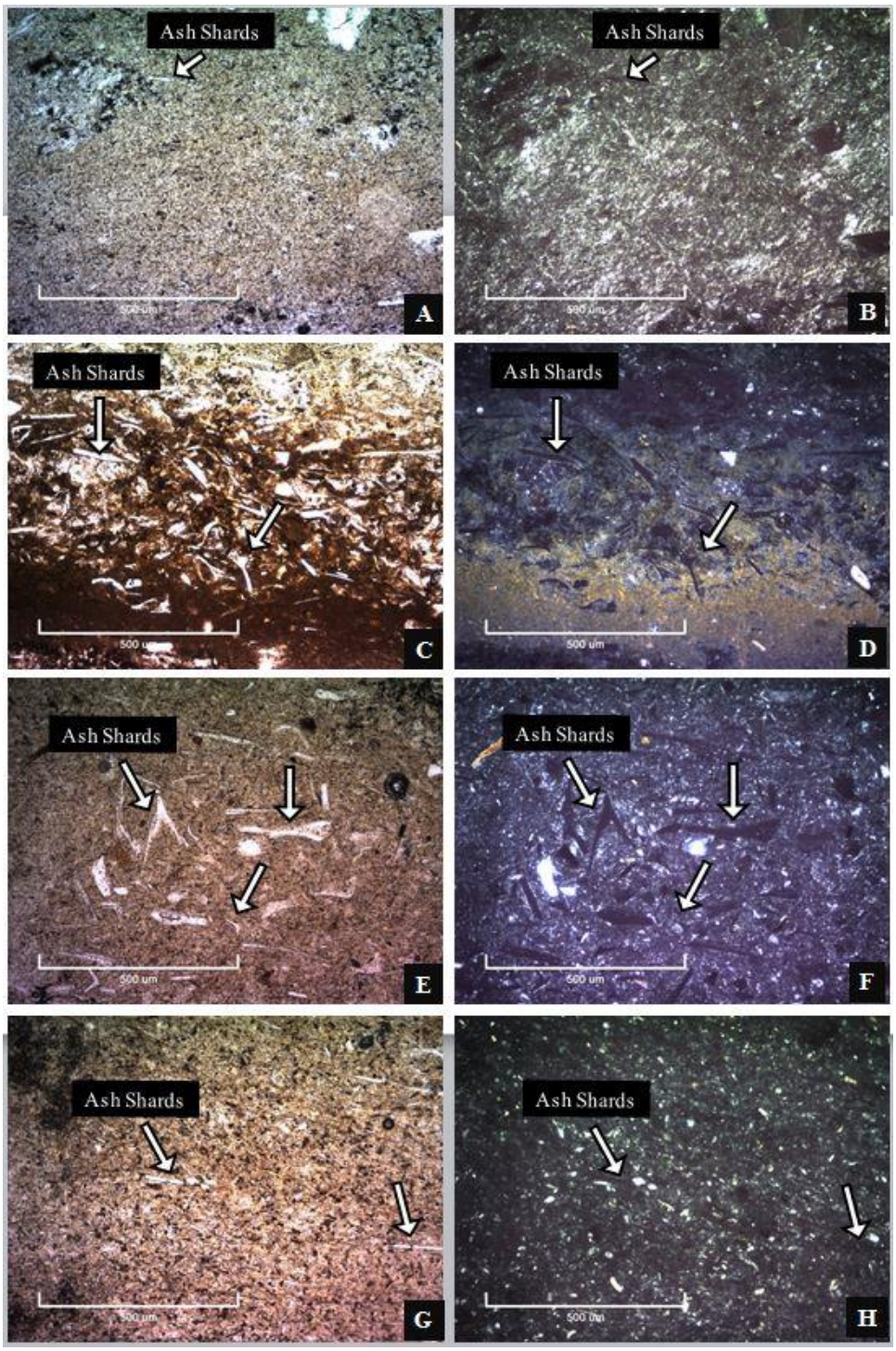

Fig. 7: Photomicrographs of the four distinct microfacies in the volcaniclastic mudstone lithofacies (Fv). A) Ashy claystone, polarized light, B) Ashy claystone, cross-polarized light, C) Ashy mudstone, polarized light, D) Ashy mudstone, cross-polarized light, E) Ashy siltstone, polarized light, F) Ashy siltstone, cross-polarized light, G) Silty ash, polarized light, H) Silty ash, cross-polarized light. A 500 μm bar is included for scale in the bottom left corner of each photomicrograph.

4.2.3. Lithofacies C (Carbonate)

Lithofacies C is the second most abundant lithofacies in the section, making up 11 of the 36 main samples and 1 of the 12 thin sections analyzed. This lithofacies is present throughout the middle of the stratigraphic section (Fig. 4). It has a single microfacies (in addition to the main lithofacies, C): sandy carbonate (Cs).

The matrix consists of carbonate and clay. Gypsum crystals are few to frequent (5-30%). Overall, carbonate (micrite with very little microspar) is dominant to very dominant (>50%) in thin sections of lithofacies C. Nevertheless, there are also laminae of sandy clay dispersed throughout. Sandy clay laminae display unistrial birefringence. This matrix appears light yellow to yellow in cross-polarized light. Sediments are strongly calcareous throughout the section. Sediment grains present include frequent (15-30%) silt and sand grains that consist of plagioclase, biotite, and volcanic ash and glassy volcanic rock fragments. Sediment grains are overall euhedral to subhedral, undulating to smooth, and subangular. Gypsum crystals are few to frequent (5-30%), with variable characteristics depending on the thin section and location.

Laminae are rare to nonexistent, appear somewhat continuous when they are present, and vary in thickness depending on the thin section and location, but overall they tend to be very thin (0.05-0.5 mm thick). Gypsum laminae display crystal orientations that are horizontal to sub-horizontal or vertical to sub-vertical locally. Very few elongate lenses of gypsum and carbonate are present.

The sediments of lithofacies C are pink to light reddish brown (5YR 6/3, 5YR 7/3) to light gray and greenish gray (10Y 6/1, 10Y 7/1) in hand samples. There is localized brown staining (10YR 6/8) and frequent (15-30%) black (10G 2.5/1) mottling.

The staining (hydrous iron oxides) is, in some places, directly associated with weathered biotite grains. This staining appears in long and thick streaks and localized fragments.

Carbonate peloids appear throughout this lithofacies, as do small opaque fragments that may be organic matter. Dissolved ostracode voids filled with calcite are present.

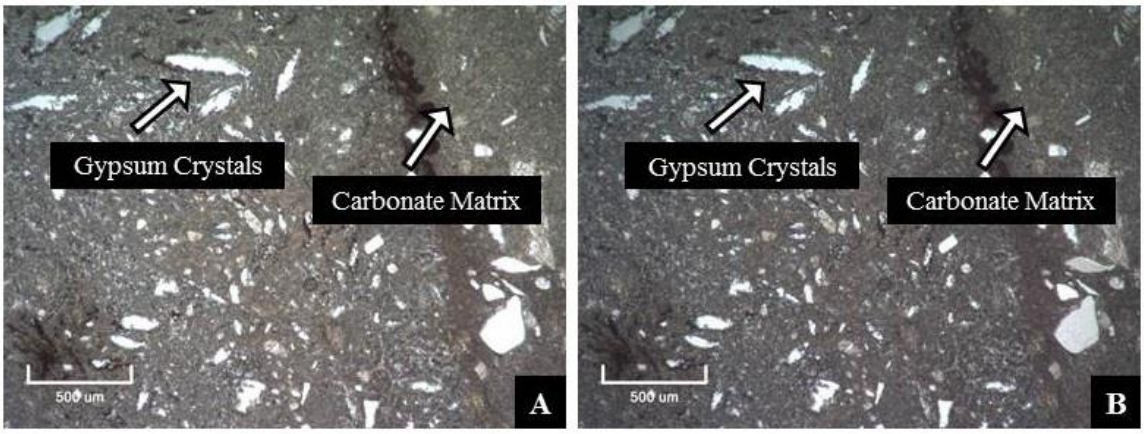

Fig. 8: Photomicrographs of the carbonate lithofacies (C). A) Carbonate, polarized light, B) Carbonate, cross-polarized light. A 500 μm bar is included for scale in the bottom left corner of each photomicrograph.

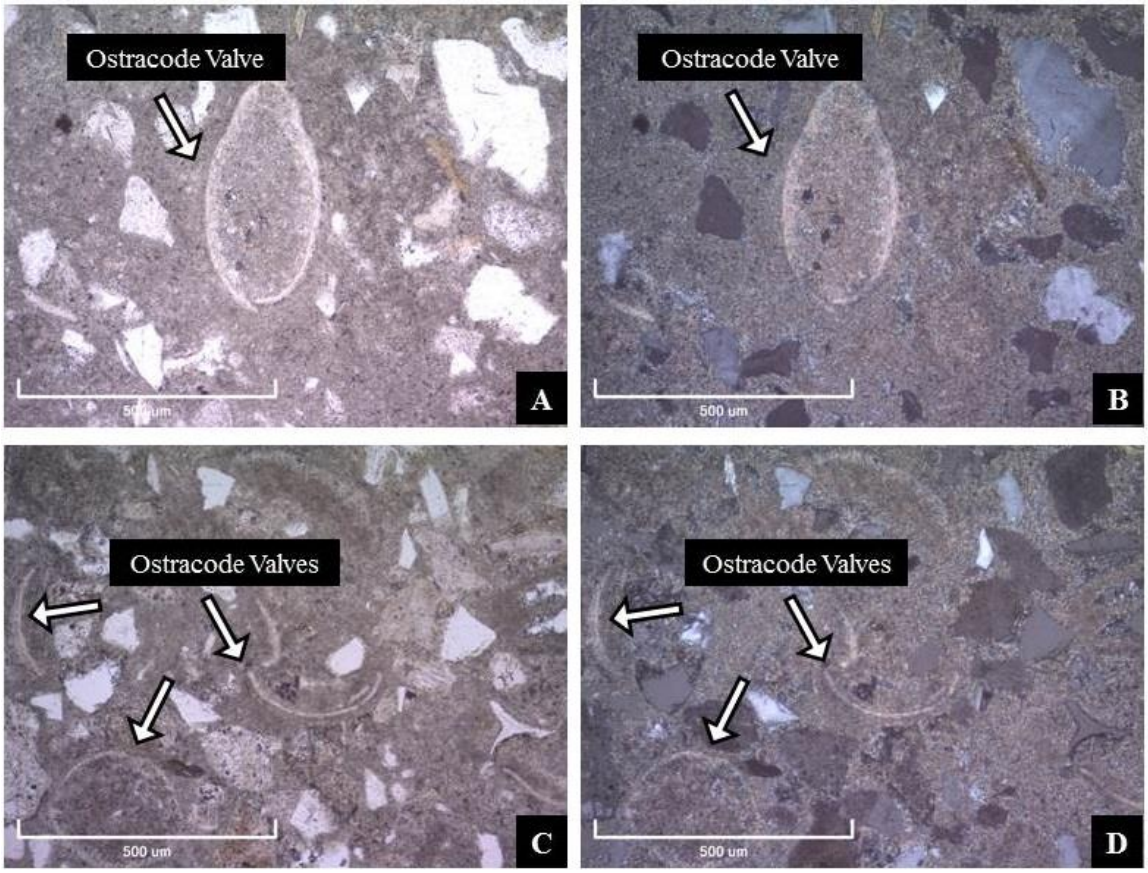

Fig. 9: Photomicrographs of ostracode valves in LB31. A) Ostracodes, polarized light, B) Ostracodes, cross-polarized light, C) Ostracodes, polarized light, D) Ostracodes, cross-polarized light. A 500um bar is included for scale in the bottom left corner of each photomicrograph.

4.2.4. Lithofacies E (Evaporite)

Lithofacies E is the second least-abundant lithofacies in the section, making up 5 of the 36 main samples and 4 of the 12 thin sections. This lithofacies is present throughout the middle of the stratigraphic section (Fig. 4). It can be subdivided into two microfacies: gypsum and carbonate (EClpon) and gypsum and claystone (EFlcvon).

The matrix consists of carbonate, clay, sand, and silt, and hand samples are typically non-fissile. Gypsum is dominant to very dominant (>50%), and the clay matrix displays unistrial birefringence. This matrix appears light yellow to yellow in cross-polarized light. Sediments vary from non-calcareous to strongly calcareous throughout

the section. Sediment grains present include frequent (15-30%) siliciclastic clay, silt, and sand. Grains in the latter two phases consist of plagioclase, biotite, olivine, hornblende, and volcanic ash and glassy volcanic rock fragments. Sediment grains are overall subhedral (frequent, 15-30%, euhedral grains are additionally present), undulating to smooth, and subangular. In some domains of thin sections, crystalline gypsum is a continuous phase that has an intergrown appearance, but elsewhere gypsum crystals exist in discrete, convoluted, and inconsistent non-parallel laminae.

Laminae are somewhat continuous to discontinuous and irregular and vary in thickness depending on the thin section and location, but overall laminae tend to be very thin to medium (0.05-3.0 mm thick). Gypsum laminae display distinct crystal orientations that are horizontal to sub-horizontal or vertical to sub-vertical locally. Very few elongate lenses of gypsum and carbonate are present.

This lithofacies is pale yellow (5Y 7/3, 8/2) in clayey and sandy zones and light and dark greenish gray (5GY 6/1, 10Y 4/1, 5/1, 6/1, 7/1, 8/1) in gypsum-dominated parts of hand samples. There is localized yellowish red and brown and reddish yellow staining (5YR 5/8, 6/8, 7.5YR 6/8, 10YR 5/8, 6/6, 7/6) and frequent (15-30%) black (10G 2.5/1) mottling. The staining (hydrous iron oxides) is, in some places, directly associated with weathered biotite grains. This staining appears in long and thick streaks and localized fragments.

In many areas, carbonate peloids appear to be compressed together, with their primary porosity filled by lenticular authigenic gypsum crystals. Rare carbonate peloids and possible filled burrows or elongate lenses appear in this lithofacies, as well as small

opaque fragments that may be organic matter. Ostracodes are present, or, more likely, dissolved ostracode voids are filled with calcite.

The gypsum and carbonate microfacies (EClpon) displays a dominant (50-70%) micritic carbonate matrix and a minor component of clay. Four subfacies (distinct lithofacies within the microfacies) occur within this microfacies: (1) 80-100% gypsum crystals and 0-20% matrix, sub-horizontally aligned, subhedral lenticular, closely packed and interlocked, (2) 40-50% gypsum crystals and 50-60% non-evaporite matrix, randomly oriented and unaligned, elongate and lenticular with a dominantly micritic carbonate matrix, (3) 90-95% gypsum crystals and 5-10% matrix, randomly oriented and aligned, variably shaped, intergrown and interlocked, and (4) 90-100% gypsum crystals and 0-10% matrix, randomly oriented and aligned, equant tabular prismatic, and intergrown. Distinct laminae, varying in thickness, of each of these subfacies are present throughout the thin sections of this microfacies. In many areas, the distinct subfacies laminae occur consecutively and in repetitive successions. Carbonate peloids and ooids are present in this microfacies; however, no organic material is present. The gypsum and clay microfacies (EFlcvon) displays a dominant (50-70%) clay matrix with a slightly silty and lesser sandy component. Very few to no biogenic structures are present, and organic material is absent.

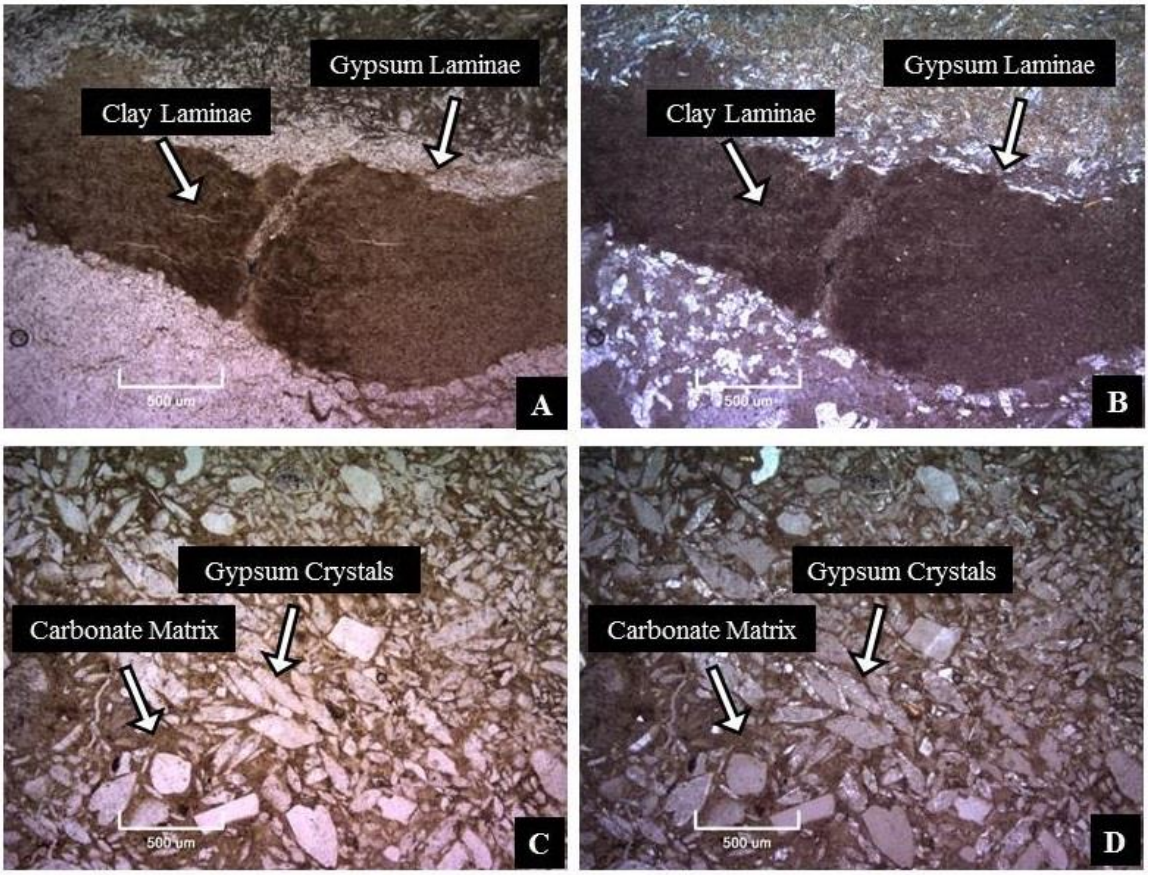

Fig. 10: Photomicrographs of the distinct microfacies in the evaporite lithofacies (E). A) Gypsum crystals and clay laminae, polarized light, B) Gypsum crystals and clay laminae, cross-polarized light, C) Gypsum crystals in carbonate matrix, polarized light, D) Gypsum crystals in carbonate matrix, cross-polarized light. A 500 μm bar is included for scale in the bottom left corner of each photomicrograph.

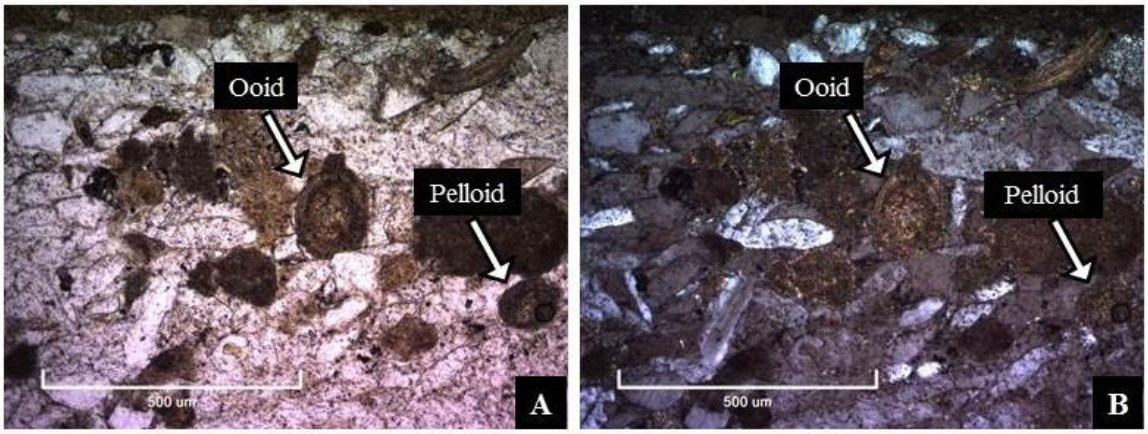

Fig. 11: Photomicrographs of a carbonate ooid and carbonate peloids in LB26. A) Ooid and peloids, polarized light, B) Ooid and peloids, cross-polarized light. A 500 μm bar is included for scale in the bottom left corner of each photomicrograph.

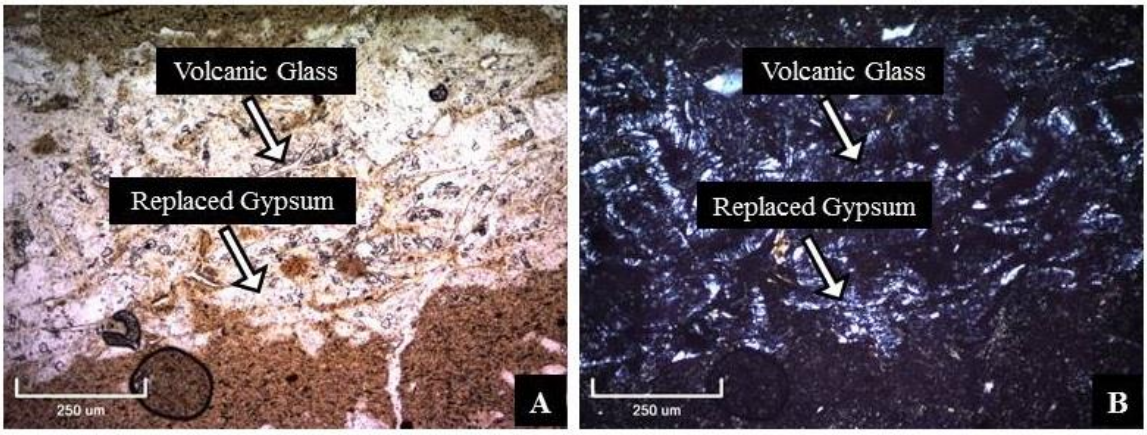

Fig. 12: Photomicrographs of volcaniclastic fragments and glass and gypsum replaced by chalcedony in LB11. A) Volcaniclastic ash fragments and glass, polarized light, B) Volcaniclastic ash fragments and glass, cross-polarized light. A 250 μm bar is included for scale in the bottom left corner of each photomicrograph.

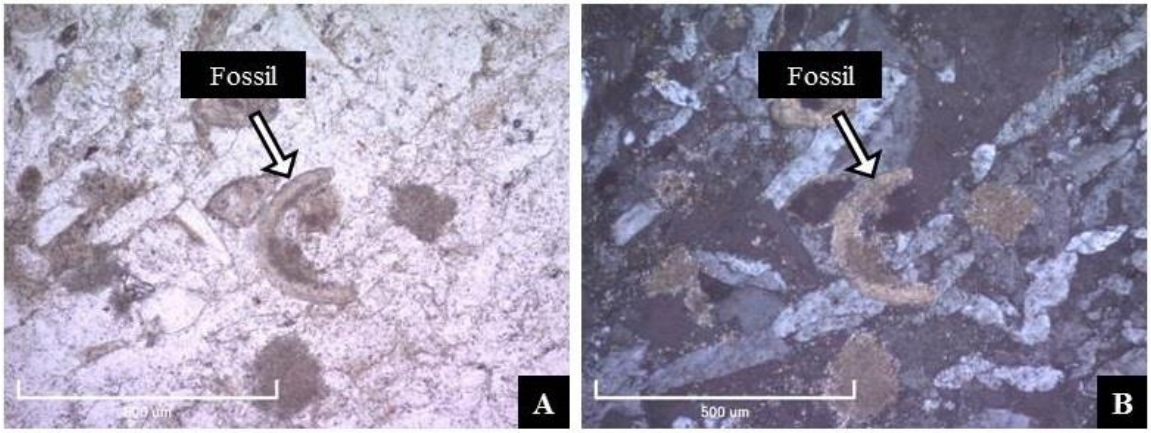

Fig. 13: Photomicrographs of fossils of unknown origin, possibly ostracode valves, in LB26. A) Fossils, polarized light, B) Fossils, cross-polarized light. A 500 μm bar is included for scale in the bottom left corner of each photomicrograph.

4.2.5. Lithofacies Sf (Muddy Sandstone)

Lithofacies Sf is one of the two least abundant lithofacies in the section, making up 4 of the 36 main samples and 2 of the 12 thin sections. This lithofacies is present throughout the stratigraphic section (Fig. 4). It can be split into two microfacies: massive (SFmv), and laminated (SFlv). One sample from this lithofacies (sample LB 5) was used to better constrain the age of the samples within the section.

The matrix consists of fine grained mud, with fine to coarse-grained sand and silt. Sediments in this lithofacies are not calcareous or are only slightly calcareous. Sediment grains present include dominant (50-70%) very fine to fine sand. Grains comprise plagioclase, sanidine, biotite and micaceous material, ferromagnesian silicate minerals (olivine, augite), and volcanic ash and glassy volcanic rock fragments (2-10% of the overall composition), and are overall euhedral to subhedral, undulating to smooth, and sub-rounded to subangular. Many clusters of euhedral gypsum crystals are partially to fully replaced by chalcedony and have lenticular tabular forms and sub-rounded outlines.

Laminae are very thin to thin (0.025-0.2 mm thick), convoluted, wavy, and non-parallel when present.

The color of lithofacies SF is generally pale yellow and brown (10YR 6/3, 6/8, 7/3 7/8, 5Y 7/3, 8/3) in hand samples, with light gray and pink (10Y 7/1, 5YR7/3) noted in a few samples. Brownish yellow (2.5Y 7/6, 5YR 5/4, 10YR 6/8) staining is present on the samples in this lithofacies, and some of the samples have black (10G 2.5/1) mottling. The staining (hydrous iron oxides) is, in some places, directly associated with weathered biotite grains. This staining appears in long and thick streaks and localized fragments.

Rare carbonate peloids and possible filled burrows or elongate lenses appear in this lithofacies.

The massive microfacies (SFmv) displays massive, randomly oriented, coarse grains that form a poorly sorted mixture of coarse components in a muddy matrix. Some biotite and micas in this microfacies exhibit “bird’s eye maple” extinction from the thin section generation, making them noticeably distinct. The laminated microfacies (SFlv) displays frequent (15-30%) discontinuous and irregular laminae present throughout.

Intact, very thin laminae of mica grains are prevalent. These laminae are oriented horizontal to sub-horizontal, with all grains oriented within 30 degrees of horizontal. Few (5-15%) elongate lenses of carbonate matrix are present.

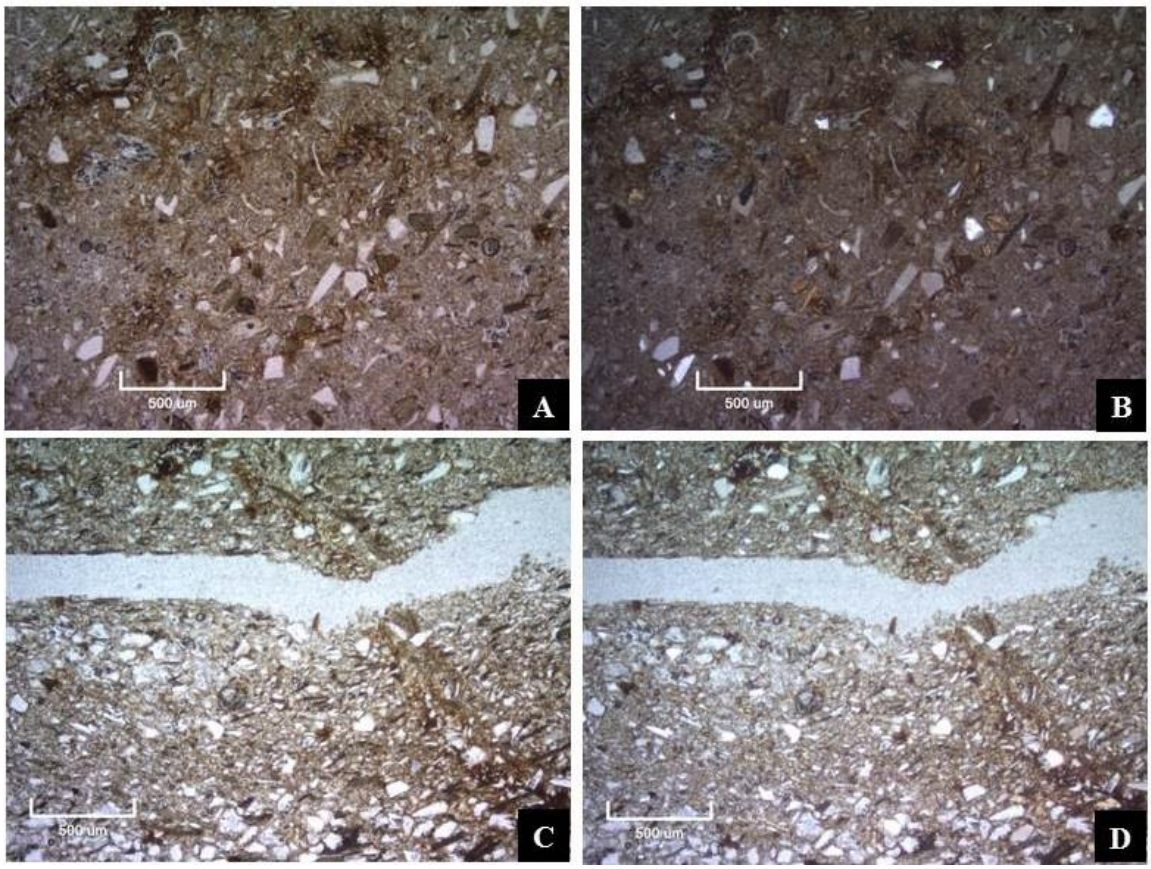

Fig. 14: Photomicrographs of the distinct microfacies in the muddy sandstone lithofacies (SF). A) Massive, polarized light, B) Massive, cross-polarized light, C) Laminated, polarized light, D) Laminated, cross-polarized light. A 500 μm bar is included for scale in the bottom left corner of each photomicrograph.

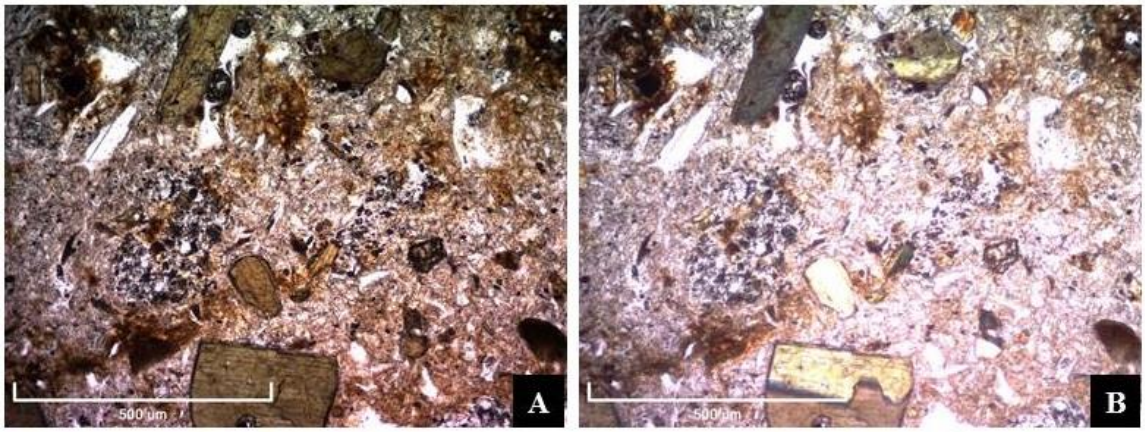

Fig. 15: Photomicrographs of ferromagnesian silicate grains in LB40. A) Ferromagnesium minerals, polarized light, B) Ferromagnesium minerals, cross-polarized light. A 500 μm bar is included for scale in the bottom left corner of each photomicrograph.

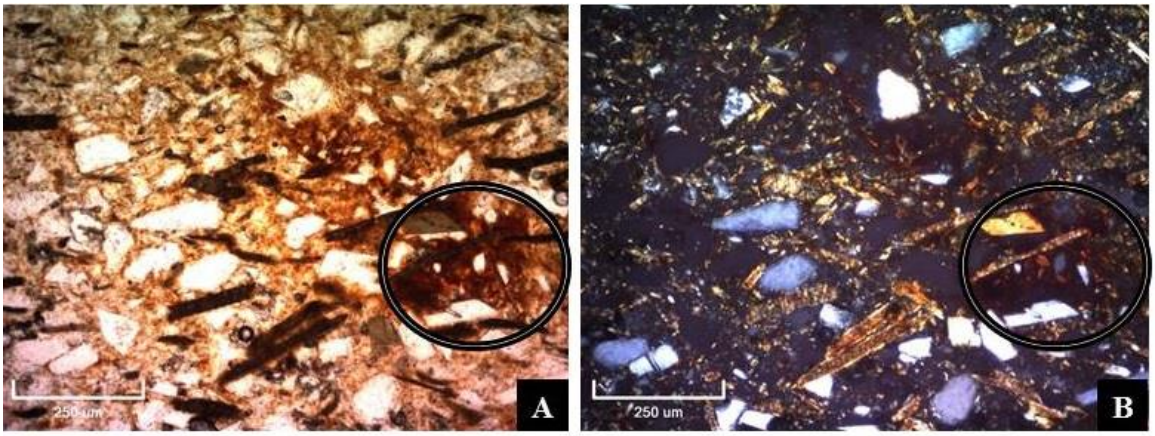

Fig. 16: Photomicrographs of staining (concentrated in the circle) in LB34, and seen throughout many of the thin sections. A) Staining, polarized light, B) Staining, cross-polarized light. A 250 μm bar is included for scale in the bottom left corner of each photomicrograph.

4.3. Geochronology

U-Pb dating of detrital zircons (Gehrels, 2014) in bounding tuffs of the outcrop provide age constraints near the top and bottom of the sedimentary succession studied. Sample LB5 is the third sample from the bottom and is dated at 5.57 ± 0.12 Ma, while sample LB36, the sixth sample from the top is dated at 5.44 ± 0.16 Ma. Gaupp et al. (1999) place these sediments in Stage 2 (shallow ephemeral lakes, playas, minor evaporite deposition, episodic sheet floods, debris flows, and tuff beds preserved)

between 6.4 to 3.7 Ma, thus late Miocene to early Pliocene. The new U-Pb detrital zircon dates are consistent with these early Stage 2 depositional ages (Kott et al., 1995).

CHAPTER 5: DISCUSSION

5.1. Depositional Environments Associated With Individual Lithofacies

The five lithofacies identified and described above are representative of distinct depositional environments, which are interpreted from rock types and sedimentary features found in each lithofacies. Table 3 presents a summary, and more detailed descriptions are provided below.

Table 3: Lithofacies and depositional environments of Lauca Basin outcrop samples. Descriptive letter code designations can be found in Table 1.

Lithofacies	Microfacies	Interpretation
Laminated mudstone (Fl)	Non-calcareous	Deposition from suspension in lacustrine environment – pelagic to littoral zone
	Calcareous	
Volcaniclastic mudstone (Fv)	Ashy siltstone	Tuffaceous lacustrine deposits – pelagic to littoral zone
	Ashy mudstone	
	Ashy claystone	
	Silty ash	
Carbonate (C)	Sandy carbonate	Intermittent deposition/precipitation of carbonate with siliciclastic sediments in a closed, ephemeral mudflat or shallow lacustrine environment
Evaporite (E)	Gypsum and carbonate	Intermittent deposition/precipitation of gypsum together with carbonate and siliciclastic sediments in a closed, ephemeral mudflat or shallow lacustrine environment
	Gypsum and clay	
Muddy sandstone (SF)	Massive	Shallow lake, possibly ephemeral
	Laminated	

5.1.1. Lithofacies Fl (Laminated Mudstone)

This lithofacies represents deposition from suspension in a lacustrine environment, likely in the central lacustrine basin (pelagic zone). Prior studies (Kott et al., 1995; Gaupp et al., 1999) note that pure claystones within Stage 2 sediments in the

Lauca Basin are extremely rare, and this is consistent with the rare occurrence of pure claystone sediments that fall in this or any other lithofacies in this study.

Samples that exhibit thin, laminated beds and a dominantly muddy matrix are indicative of an environment in which fine sediments could settle from suspension, with little to no impact of wave action or current, and an inactive or nonexistent benthic community, as indicated by the lack of bioturbation and intact planar parallel laminae. There is no evidence of *in situ* vascular plants. The laminae indicate seasonal or periodic changes in sediment source that resulted in variation in the deposition of carbonate materials relative to clastic materials, and the lack of bioturbation indicates seasonal stratification, high salinity, or both (Finkelstein et al., 1999).

Samples that exhibit convoluted, wavy non-parallel laminae, or localized, lenticular laminae suggest deposition in a shallower paleolake where sediments were affected by wave action (Allen, 1981; Alfaro et al., 1997; Martel and Gibling, 2009; Andrews et al., 2016). The persistence of laminae, although convoluted, wavy, and non-parallel, indicates continued seasonal or periodic changes in sediment source that resulted in variation in the deposition of carbonate materials relative to clastic materials.

The euhedral gypsum crystals dispersed throughout the matrix in this lithofacies indicate the crystallization of an evaporate phase in the sediment, most likely by growth within the sediment after deposition associated with episodic water-table decline, rather than precipitation and fallout from the water column (Bowler and Teller, 1986; Rosen and Warren, 1990; Mees, 1999b; Orti et al., 2003). Most of the gypsum in this lithofacies has been partially to fully replaced by chalcedony. The replacement of gypsum by chalcedony occurs in silica-rich high-pH early-diagenetic settings of saline lakes (Orti et

al., 1997; Gilbert et al., 2007). The abundant rhyolitic and dacitic volcanic ash deposited in the surrounding area would have provided ample silica, and high pH is consistent with a saline paleolake during or following the formation of evaporite crystals (Kott et al., 1995; Bowman and Sachs, 2008). Another potential source of silica for this process is the abundant diatom-rich material or diatom skeletons directly (Gilbert et al., 2007).

The mud pellets that are present in variable amounts throughout this lithofacies possibly represent an aeolian component contributed to the basin during more arid conditions via wind either through direct wind-blown deposition into water and associated fallout or erosion of dunes and subsequent sweeping deposition (either by wind or runoff) into the lake (Bowler and Teller, 1986). It is possible that much of the finer sediment deposited in this lithofacies was through aeolian processes, as fine-grained sediments in the surrounding arid environment were likely loose and poorly lithified. These types of sediments would have been transported onto the paleolake surface and settled out from suspension. It is also possible that the presence of mud pellets in this lithofacies are of biotic origin. Fecal pellets that resemble mud pellets are excreted by a number of lacustrine organisms (Freytet and Verrecchia, 2002).

Red to dark red staining is present throughout and likely the result of weathering of biotite and resulting hydrous oxide staining. This occurred through chemical weathering and oxidation of Fe^{2+} to Fe^{3+} in the biotite. Biotite was likely supplied via volcanic activity and its resulting volcaniclastic contribution to the sediments. Biotite is common in arid regions and in riverine supplied sediments that erode bedrock originally with high micaceous compositions (Bisdom et al., 1982). The weathering pigment generated by the oxidation of iron in the biotite present, referred to in this study as

"staining", further supports the indication that many of the volcaniclastic materials in this succession have weathered or begun weathering to smectitic clays (Bisdom et al., 1982). When appearing in streaks, this staining can indicate the grain boundaries that have cracked and opened as a result of weathering (Irfan, 1999). These streaks will tend to preferentially follow the microcracks as they form.

This lithofacies overall appears to represent a deeper depositional environment than that associated with other lithofacies in this study.

5.1.2. Lithofacies Fv (Volcaniclastic Mudstone)

This lithofacies is interpreted as Tuffaceous lacustrine deposits. Volcanic material in this lithofacies is interpreted as a tuffaceous horizon or distinctive beds of lithified volcanic ash, and the material largely is not welded, with no evidence of deposition by pyroclastic surges. One sample from this lithofacies (sample LB 36) was used to better constrain the age of the samples within the section and enables the correlation of this section to major volcanic events documented previously in the region.

This lithofacies was likely deposited under conditions similar to those of lithofacies Fl, as evidenced by the laminated beds and muddy and fine-grained matrix. The key difference is that lithofacies Fv has a significant amount of volcanic material, composed of aphanitic dacitic and rhyolitic materials. This is indicated by the mineral composition (dominantly felsic quartz and plagioclase feldspar with frequent mafic phenocrysts including hornblende, olivine, and biotite), texture (aphanitic microcrystalline components with blocky plagioclase phenocrysts, sub-rounded to corroded quartz phenocrysts, and subhedral elongated hornblende and biotite), and

general appearance (light colored and fine grained; Díaz et al., 1999; Gaupp et al., 1999; Bowman and Sachs, 2008; de Wet et al., 2015).

The subhedral gypsum grains that are present in this lithofacies suggest formation of evaporitic material in interstitial spaces within the matrix and are most likely a product of subaqueous precipitation in the sediments (Bowler and Teller, 1986; Rosen and Warren, 1990; Mees, 1999b; Orti et al., 2003). Red to dark red staining is present throughout and, as described above for lithofacies F1, is likely the result of chemical weathering of biotite and resulting hydrous oxide staining.

This lithofacies overall appears to represent a relatively deep depositional setting as compared with C, E, and SF in this study (see below).

5.1.3. Lithofacies C (Carbonate)

This lithofacies is formed from the precipitation and deposition of carbonate together with siliciclastic sediments in a closed-basin lake. Carbonate deposition is commonly microbially mediated and facilitated by evaporative concentration of lake water (Anadon et al., 2009; Tucker and Wright, 2009). The presence of gypsum along with abundant carbonate indicates a depositional environment in which evaporation exceeded precipitation and surface runoff. Alternating carbonate and gypsum laminae represent periods of lake dilution and concentration, respectively, associated with variation in evaporation relative to precipitation and surface runoff (Orti et al., 2003). Evidence of desiccation cracking and the appearance of auto-brecciation or nodularization in this lithofacies support the interpretation of a shallow lake or a mudflat that experienced episodic subaerial exposure, and the abundant carbonate sediment indicates lesser influx of siliciclastic sediment into the basin.

There is no evidence of in-situ vegetation, and laminae are rare. The non-fissile nature of many of these sediments could result from several processes: (1) bioturbation could have disturbed the orientation of clay minerals, keeping them from their preferred orientation; (2) the content of actual clay minerals within the rock was relatively lower than other components; (3) the flocculation of clay minerals caused them to lack preferential orientation due to increased salinity and/or organic matter in the water; or (4) the recrystallization of clay minerals during diagenesis caused them to lack preferential orientation (Byers, 1974; Curtis et al., 1980; Moon and Hurst, 1984). The abundant carbonate and gypsum in the sediments are indicative of moderate to high salinity, and petrographic analysis of thin sections showed little evidence of bioturbation - clay components tended to be preferentially oriented and are a significant component in the makeup of the lithofacies matrix. Thus, flocculation due to increased salinity is the more likely explanation for the non-fissile nature of this lithofacies. The lack of laminations also suggests few or none cyclic changes in inflow. In other words, sediments in lithofacies C were most likely deposited in a lacustrine environment with little to no hydrologic input or output other than evaporation and occasional precipitation.

The presence of ostracodes indicates a shallow, carbonate-rich paleolake with high levels of oxygen and light (Perez et al., 2002). Because they appear to have been dissolved and filled with another material, they support the hypothesis that the absence of fossils within most of the lithofacies was due to diagenetic dissolution (Kott et al., 1995; Gaupp et al., 1999; Williams et al., 2008). Diagenesis may also be the cause of the absence of other organic material within most of the lithofacies.

As described for other lithofacies, the euhedral gypsum grains dispersed throughout the matrix suggest post-depositional formation of evaporitic material in the sediments, and the replacement of gypsum by chalcedony suggests a silica-rich high-pH environment. The red to dark-red staining is likely the result of chemical weathering of biotite supplied by regional volcanism and the resulting hydrous oxide staining.

This lithofacies overall appears to represent shallower conditions relative to those of lithofacies Fl and Fv, with alternations is salinity driven by changes in the balance of evaporation relative to precipitation.

5.1.4. Lithofacies E (Evaporite)

This lithofacies is interpreted as intermittent precipitation and deposition of evaporates together with carbonate and siliciclastic sediments in a closed shallow lake or ephemeral mudflat in which evaporation exceeded precipitation and surface runoff. Alternating carbonate and gypsum laminae represent periods of lake dilution and concentration, respectively (Orti et al., 2003). Modern-day evaporite-producing environments commonly occur in closed-basin systems in arid climates (Warren, 2010). Evidence of desiccation cracks support the interpretation that water levels periodically declined to produce an ephemeral mudflat.

The ooids present in this lithofacies are all concentric tangential (Richter, 1983). The carbonate ooids and peloids indicate a shallow and high-energy environment (Reijers and Ten, 1983). Lacustrine ooids of this type have been shown to be affected by, and sometimes dependent on, higher salinities, coupled with the shallow water and high agitation necessary for ooid formation (Davies et al., 1978; Popp and Wilkinson, 1983; Richter, 1983). The appearance of concentric tangential ooids versus radial ooids

indicates an environment with bed load transport, high energies, and frequent abrasion (Heller et al., 1980).

Gypsum can be formed via a few key mechanisms as a subaqueous precipitate (lacustrine deposits, synsedimentary gypsum) or by subaerial evaporation-based processes after lake desiccation (wet or dry mudflat system deposits, diagenetic gypsum) (Mees et al., 2012). Further, gypsum can be affected by water movement upwards through capillary rise (common in very arid climates) and water movement downwards through limited leaching, where soil is not fully wetted and lacustrine deposit inherited gypsum is therefore not removed (common in moderately arid climates) (Jafarzadeh and Burnham, 1992).

Subaqueous precipitate gypsum is often recognizable by its variation in crystal morphology, crystal size, and gypsum content; evidence of grading (normal or inverse) and vertical change in morphology; horizontal alignment of crystals (which can also indicate aeolian depositional processes); and dominantly lenticular shaped crystals (Chen et al., 1991; Orti et al., 2003; Mees et al., 2012). Growth of gypsum crystals in the water column tends to produce prismatic (parallel or tabular) habits, dominantly matrix-free, and equant in shape (Bowler and Teller, 1986).

Subaerial precipitate gypsum is commonly zoned. Lenticular shaped crystals that are not recognizably aligned or bedded, or crystal deposits that display abrupt variations in morphology, indicate either diagenetic subaerial formation processes or subaqueous synsedimentary deposits that have been altered or modified (Mees et al., 2012). Gypsum crystals dispersed in a matrix are generally thought to be subaerial deposits, however, subaqueous inter-sediment gypsum formation in lacustrine benthic zones also can

produce matrix-dominant gypsum deposits (Bowler and Teller, 1986; Rosen and Warren, 1990; Mees, 1999b; Orti et al., 2003).

As noted above, multiple gypsum subfacies (distinct lithofacies within the microfacies) occur within this microfacies: (1) 80-100% evaporite crystals and 0-20% matrix, sub-horizontally oriented, subhedral lenticular, closely packed and interlocked; (2) 40-50% evaporite crystals and 50-60% matrix, randomly oriented and unaligned, elongate and lenticular with a dominantly micritic carbonate matrix; (3) 90-95% evaporite crystals and 5-10% matrix, randomly oriented and aligned, variably shaped, intergrown, and interlocked; and (4) 90-100% evaporite crystals and 0-10% matrix, randomly oriented and aligned, equant tabular prismatic, and intergrown and interlocked. Although tentative generalizations can be made about the depositional environments of each of these on the basis of the crystal morphologies, gypsum morphologies alone are insufficient to interpret paleoenvironments and must be supplemented by supporting data and observations.

Subfacies (1) is indicative of a subaqueous precipitate gypsum-forming environment, in which the dominant gypsum crystals formed in the water column and precipitated out into uniformly aligned, closely packed, and interlocked lenticular beds. Subfacies (2) is indicative of a subaerial precipitate gypsum-forming environment, in which lenticular gypsum authigenically grew in interstitial spaces within the matrix. Subfacies (3) is indicative of a subaerial precipitate gypsum-forming environment, in which gypsum crystals formed in interstitial spaces and were shaped accordingly. Subfacies (4) is indicative of a subaqueous precipitate gypsum-forming environment, in which equant tabular-prismatic gypsum crystals formed in the water column and

precipitated out in varying beds. Other samples from the evaporite and clay microfacies are indicative of a subaerial precipitate gypsum-forming environment, in which gypsum crystals authigenically grew in interstitial spaces within the matrix. The closely alternating gypsum beds with variable characteristics indicate a cycle between marginal depositional environments, from ephemeral mudflat (dominantly subfacies (2), (3), and the evaporite and clay matrix) to shallow lacustrine (dominantly subfacies (1) and (4)) (Screiber and Tabakh, 2000). Some of the gypsum in this lithofacies has been partially to fully replaced by chalcedony, suggesting a silica-rich high-pH lake.

There is no evidence of in-situ vegetation (possibly due to disappearance of evidence via oxidation), and inconsistent laminae are present in many samples. Many of the samples also display a dominant non-fissile nature, which is consistent with the inferred high-salinity environment (abundant gypsum and carbonate), as discussed above. Red to dark red staining is present throughout and is likely the result of chemical weathering of biotite and resulting hydrous oxide staining.

This lithofacies overall appears to represent deposition in either an ephemeral mudflat or a shallow paleolake. Overall it is most similar to lithofacies C.

5.1.5. Lithofacies Sf (Muddy Sandstone)

This lithofacies is interpreted as a shallow, possibly ephemeral, lake. This lithofacies overall appears very immature due to the diverse composition of grains distributed throughout, the dominant plagioclase and quartz content, and varying textures. Many grains tend to be poorly rounded to sub-rounded, indicating moderate transport and immaturity. Sediments in this lithofacies were likely deposited as a result of the winnowing away of the finest-grained materials in the moderately high-energy

environment typical of shallower regions of a lake. The presence of subhedral, subangular to sub-rounded grains, very discontinuously and irregularly to not laminated, dominantly muddy sandstone with common evaporite minerals indicates an ephemeral saline lacustrine environment, likely shallower than that of other lithofacies in this study (Hardie et al., 1978).

The convoluted, wavy, and non-parallel laminae present in some samples of this lithofacies indicate that the depositional processes were affected by mild wave action within the paleolake. Thus, the site may have been in the littoral zone, although somewhat more distal environments are possible depending on the extent of the paleolakes wave action and wave base (Martel and Gibling, 2009; Andrews et al., 2016). The absence of bioturbation or evidence of *in situ* vegetation continues to demonstrate that the sediments either were not affected by the activities of littoral organisms, or alternately that oxidation destroyed organic remains.

Massive textures in sandstone can represent a number of depositional environmental indicators. Possibilities include sediment gravity flows, including small-scale lacustrine turbidites induced by either rare precipitation events, or aeolian processes, and the presence of some convoluted laminae structures supports rapid deposition (Sturm and Matter, 1978; Andrews and Hartley, 2015). Post-depositional pedogenic processes may have also destroyed laminae in samples with a largely massive texture (Benavente et al., 2015).

The euhedral gypsum grains that are dispersed throughout the matrix in this lithofacies indicate formation of evaporitic material in sediment post-deposition, and some of the gypsum in this lithofacies has been partially to fully replaced by chalcedony,

indicating a silica-rich high-pH lake. Red to dark red staining is present throughout and likely the result of chemical weathering of biotite and resulting hydrous oxide staining.

This lithofacies overall appears to represent deposition in a shallow paleolake.

5.2. Paleoenvironmental History

Alternation between lithofacies within the sedimentary section suggests variation in lake depth and lake chemistry through time. A graph illustrating inferred changes in depositional environments was generated using "paleoenvironmental indicators" of 1 through 4, assigned based on inferred deeper to shallower conditions respectively. Lithofacies Fl and Fv were categorized with an indicator value of "4," due to evidence consistent with deeper conditions at the site (evidence of stratification and the dominantly fine, settled-from-suspension grain sizes). Yet there is evidence of intervals of relatively shallower conditions in some lithofacies Fl samples (mud pellets), suggesting some variation through time. Lithofacies C and E were categorized with an indicator value of "3" and "2," respectively. Both lithofacies C and E may represent paleolake depths from shallow lacustrine to ephemeral mudflat environments based on their mineral morphology and modern examples of carbonate and gypsum formation. Lithofacies SF was categorized with an indicator value of "1," based on the interpretation of a shallow, possibly ephemeral, lacustrine environment. This classification enables a visualization of inferred paleoenvironmental transitions in water depth, which may reflect variation between wetter and drier environments with ascension through the stratigraphic section.

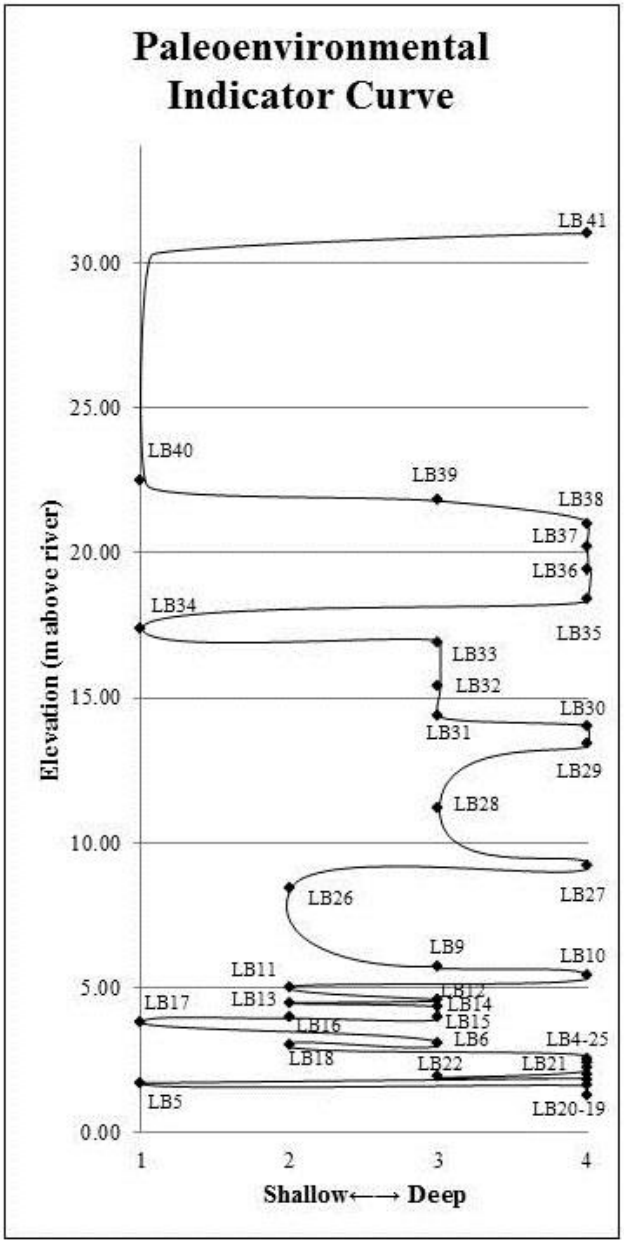

Fig. 17: Paleoenvironmental indicator curve illustrating relative transitions between shallow and deep environments with ascension through the stratigraphic section.

Fluctuations between lithofacies occur in a cyclic higher frequency manner in the lower section, lengthening into more expanded progressions with succession through the middle and upper section. Assuming relatively stable sediment accumulation rates, this indicates shorter environmentally stable periods of deposition in the lower section and more prolonged environmentally stable periods of deposition in the middle and upper

section. Fig. 17 suggests that the lake was deep, or moderately deep, for most of the section, with only four intervals of the shallowest paleoenvironmental indicator, 1 (lithofacies SF). The gypsum crystal morphologies suggest that many units with evaporite components weren't necessarily formed in subaerial conditions and that lacustrine conditions were persistent during the deposition of almost the entire section. The succession of evaporites and carbonates throughout the section, especially concentrated in the middle fourteen meters, indicates arid conditions throughout, coupled with repeated basin restriction, and the variation in gypsum morphology indicates marginal, mixed shallow-subaqueous and subaerial depositional environments (Schreiber and Tabakh, 2000; Schroder et al., 2003).

Compared with other paleoenvironmental work in the region, these data indicate that the Lauca Basin experienced more consistently lacustrine environments than was common elsewhere in the region at the time (Kott et al., 1995; Gaupp et al., 1999; Saez et al., 1999; Bao et al., 1999; Mpodozis et al., 2005). Basins within the northern Chilean Altiplano (roughly between 23˚-30˚S) were under the influence of a steady high-pressure southeastern Pacific cell during the Neogene and likely would have experienced arid to semiarid conditions similar to those of the Lauca Basin (Parrish et al., 1982; Parrish and Curtis, 1982). Transitions between ephemeral, evaporate-dominated lacustrine systems and perennial non-evaporitic systems were common in regionally similar basins (Bao et al., 1999; Saez et al., 1999; Mpodozis et al., 2005; Placzek et al., 2009). The Quillagua-Llamara Basin, in the northern Chilean Altiplano (approximately 21˚-23˚S, 69˚-70˚W, ~1000 masl) with Neogene age sediment fill, was more heavily influenced by fluvial freshwater inputs and likely was less saline than the paleolacustrine system in the Lauca

Basin. Yet seasonal variations in deposition are present in both, suggesting regional variability in aridity (Bao et al., 1999; Saez et al., 1999). Oligocene to Pliocene sediment fill from the Salar de Atacama Basin and other smaller Atacama Desert basins (approximately 22˚-24˚S, 68˚-69˚W, ~3000 masl) is dominantly evaporite-rich and endorheic lacustrine in nature and has similar felsic volcaniclastic sediments to those of the Lauca Basin (Mpodozis et al., 2005; Placzek et al., 2009).

Following the deposition of the Lauca Basin stratigraphic section, prior studies suggest that the Lauca Basin experienced increasing aridity and cooling, similar to global and regional paleoclimate patterns during the Miocene-Pliocene transition. This was followed by a period of semi-humid conditions, increased precipitation and runoff, and a transition to local fluvial environments that differed from the lacustrine environments of earlier periods (Gaupp et al., 1999; Zachos et al., 2001; Wara et al., 2005). Cooling and the increase in humidity during this subsequent period were associated with increased glaciation in South America (Mercer, 1984).

The overlying Lauca Ignimbrite, dated at 2.3 ± 0.7 Ma, is widespread in the region and indicates more prominent volcanic activity in nearby volcanic chains during the period following deposition of this section (Schroder and Worner, 1995, 1996; Charrier et al., 2004; Garcia et al., 2011). Within the Lauca Basin, Lauca Ignimbrite beds show little to no evidence of having been deposited in extensive water bodies, indicating that the basin had transitioned to fluvial or shallow perennial to ephemeral lacustrine environments at this time (Gaupp et al., 1999). Remains of the Lauca Ignimbrite are documented in valley bottoms in the Coastal Cordillera and western Central Depression,

and on terraces in the eastern Central Depression and the Precordillera, indicating that most fluvial dissection occurred prior to their deposition (Garcia et al., 2011).

Lauca Formation sediments were never deeply buried post-deposition, as demonstrated by the rare point contacts, loose compaction, and poor lithification of many units. Minor diagenetic processes affected Lauca Formation sediments, as is seen in the silicification of many of the gypsum crystals in our samples and noted in previous studies, the apparent weathering of volcaniclastic materials into smectitic clays, and the staining and mottling present in most samples (Kott et al., 1995).

The high resolution sequence analyzed using sedimentological and petrographic methods in this thesis demonstrates that the Lauca Basin, in the late Miocene to early Pliocene, was characterized by a series of changes in lake depth in a persistently saline lake, in an arid environment. Results supplement those of previous studies, providing a more comprehensive paleoenvironmental regional history (Kott et al., 1995, Gaupp et al., 1999).

CHAPTER 6: CONCLUSION

This thesis extends the paleoenvironmental and geological evaluations of Kott et al. (1995) and Gaupp et al. (1999) by providing an analysis of basin history at higher temporal resolution. Additionally, new geochronological tools, specifically detrital zircon geochronology on bounding tuffaceous samples, facilitated the production of a well-constrained regional history. This detailed lithofacies scheme based on sedimentary and petrographic analyses indicates that the Lauca Basin of northern Chile experienced a variety of paleoclimatic changes, as discussed above. This environment was influenced

strongly by evaporation and precipitation, with significantly lesser influences of volcanism, tectonism, and sedimentary supply. The bulk of sediments deposited in the sedimentary section were formed in a saline, occasionally ephemeral lake under arid, and dominantly evaporation controlled, environment.

REFERENCES

Alfardo, P., Moretti, M., Soria, J.M., 1997, Soft-sediment deformation structures induced by earthquakes (seismites) in Pliocene lacustrine deposits (Guadix-Baza Basin, Central Betic Cordillera): Eclogae Geologicae Helvetiae, v. 90, p. 531-540.

Allen, P.A., 1981, Wave-generated structures in the Devonian lacustrine sediments of south-east Shetland and ancient wave conditions: Sedimentology, v. 28, i. 3, p. 369-379.

Alonso, R.N., Viramonte, J.G., 1990, Borate deposits in the Andes: Stratabound Ore Deposits in the Andes, v. 8, p. 721-732.

Anadon, P., Cabrera, L., Kelts, K, 2009, Lacustrine carbonates: facies models, facies distributions and hydrocarbon aspects: Lacustrine Facies Analysis, ch. 3.

Andrews, S.D., Hartley, A.J., 2015, The response of lake margin sedimentary systems to climatically driven lake level fluctuations: Middle Devonian, Orcadian Basin, Scotland: Sedimentology, v. 62, i. 6, p. 1693-1716.

Andrews, S.D., Moreau, J., Archer, S., 2016, Devonian lacustrine shore zone architecture: giving perspective to cliff exposures with ground penetrating radar: Sedimentology, v. 63, p. 2087-2105.

Bao, R., Saez, A., Servant-Vildary, S., Cabrera, L., 1999, Lake-level and salinity reconstruction from diatom analyses in Quillagua Formation (late Neogene, Central Andean forearc, northern Chile): Paleogeography, Paleoclimatology, Paleoecology, v. 153, p. 309-335.

Batenburg, S., Reichart, G.J., Jilbert, T., Janse, M., Wesselingh, F., Renema, W., 2011, Interannual climate variability in the Miocene: high resolution trace element and stable isotope ratios in giant clams: Paleogeography, Paleoclimatology, Paleoecology, v. 306, p. 75-81.

Benavente, C., Mancuso, A., Cabaleri, N., Gierlowski-Kordesch, E., 2015, Comparison of lacustrine successions and their palaeohydrological implications in two sub-basins of the Triassic Cuyana rift, Argentina: Sedimentology, v. 62, p. 1771-1813.

Billups, K., 2002, Late Miocene through early Pliocene deep water circulation and climate change viewed from the sub-Antarctic South Atlantic: Palaeogeography, Palaeoclimatology, Palaeoecology, v. 185, no. 3-4, p. 287-307.

Bisdom, E.B.A., Stoops, G., Delvigne, J., Altemuller, H.J., 1982, Micromorphology of weathering biotite and its secondary products: Pedologie, v. 32, i. 2, p. 225-252.

Bowler, J.M., Teller, J.T., 1986, Quaternary evaporates and hydrological changes, Lake Tyrrell, North-West Victoria: Australian Journal of Earth Sciences, v. 33, p. 43-63.

Bowman, J., Sachs, J., 2008, Chemical and physical properties of some saline lakes in Alberta and Saskatchewan: Saline Systems, v. 4:3.

Brierley, C.M, Fedorov, A.V., Liu, Z., Herbert, T.D., Lawrence, K.T., LaRiviere, J.P., 2009, Greatly expanded tropical warm pool and weakened Hadley circulation in the Early Pliocene: Science, v. 323, no. 5922, p. 1714-1718.

Bullock, P., Fedoroff, N., Jongerius, A., Stoops, G., Tursina, T., Babel, U., 1985, Handbook for Soil Thin Section Description.

Byers, C.W., 1974, Shale fissility: relation to bioturbation: Sedimentology, v. 21, i. 3, p. 479.

Cembrano, J., Lavenu, A., Yañez, G., Riquelme, R., García, M., González, G., Hérail, G., 2007, Neotectonics. In: Gibbons, W., Moreno, T. (Eds.), The Geology of Chile: The Geological Society of London, p. 231-261.

Charrier, R., Chavez, A., Elgueta, S., Herail, G., Flynn, J., Croft, D., Wyss, A., Riquelme, R., Garcia, M., 2004, Rapid tectonic and paleogeographic evolution associated with the development of the Chucal anticline and the Chucal-Lauca Basin in the Altiplano of Arica, northern Chile: Journal of South American Earth Sciences, v. 19, p. 35-54.

Chen, X.Y., Bowler, J.M., Magee, J.W., 1991, Aeolian landscapes in central Australia: gypsiferous and quartz dune environments from Lake Amadeaus: Sedimentology, v. 38, p. 519-538.

Curtis, C.D., Lipshie, S.R., Oertel, G., Pearson, M.J., 1980, Clay orientation in some Upper Carboniferous mudrocks, its relationship to quartz content and some inferences about fissility, porosity and compactional history: Sedimentology, v. 27, i. 3, p. 333-339.

Davies, P.J., Bubela, B., Ferguson, J., 1978, The formation of ooids: Sedimentology, v. 25, i. 5, p. 703-730.

de Wet, C.B., Godfrey, L., de Wet, A.P., 2015, Sedimentology and stable isotopes from a lacustrine-to-palustrine limestone deposited in an arid setting, climatic and tectonic factors: Miocene – Pliocene Opache Formation, Atacama Desert, Chile: Palaeogeography, Palaeoclimatology, Palaeoecology, v. 426, p. 46-67.

Díaz, G.C., Mendoz, M., García-Veigas, J., Pueyo J.J., Turner, P., 1999, Evolution and geochemical signatures in a Neogene forearc evaporitic basin: the Salar Grande (Central Andes of Chile): Palaeogeography, Palaeoclimatology, Palaeoecology, v. 151, p. 39-54.

Fedorov, A.V., Brierley, C.M., Emanuel, K., 2010, Tropical cyclones and permanent El Niño in the early Pliocene epoch: Nature, v. 463, no. 7284, p. 1066-1070.

Finkelstein, D.B., Hay, R.L., Altaner, S.P., 1999, Origin and diagenesis of lacustrine sediments, upper Oligocene Creede Formation, southwestern Colorado: GSA Bulletin, v. 111, i. 8, p. 1175-1191.

Freytet, P., Verrecchia, E., 2002, Lacustrine and palustrine carbonate petrography: an overview: Journal of Paleolimnology, v. 27, i. 2, p. 221-237.

Galeotti, S., Heydt, A., Huber, M., Bice, D., Dijkstra, H., Jilbert, T., Lanci, L., Reichart, G.J., 2010, Evidence for active El Niño Southern Oscillation variability in the late Miocene greenhouse climate: Geology, v. 38, p. 419-422.

Garcia, M., Riqelme, R., Farias, M., Herail, G., Charrier, R., 2011, Late Miocene-Holocene canyon incision in the western Altiplano, northern Chile: tectonic or climatic forcing?: Journal of the Geological Society, v. 168, p. 1047-1060.

Gaupp, R., Kött, A., Wörner, G., 1999, Palaeoclimatic implications of Mio – Pliocene sedimentation in the high-altitude intra-arc Lauca Basin of northern Chile: Palaeogeography, Palaeoclimatology, Palaeoecology, v. 151, p. 79-100.

Gehrels, G.E., 2014, Detrital zircon U-Pb geochronology applied to tectonics: Annual Review of Earth and Planetary Sciences, v. 42, p. 127-149.

Gierlowski-Kordesch, E.H., Kelts, K., 2000, Lake basins through space and time: AAPG Studies in Geology, v. 46, p. 648.

Gilbert, L., Orti, F., Rosell, L., 2007, Plio-Pleistocene lacustrine evaporates of the Baza Basin (Betic Chain, se Spain): Sedimentary Geology, v. 200, p. 80-116.

Hardie, L.A., Smoot, J.P., Eugster, H.P., 2009, Saline lakes and their deposits: a sedimentological approach: Modern and Ancient Lake Sediments, ch. 2.

Haug, G., Tiedemann, R., 1998, Effect of the formation of the Isthmus of Panama on Atlantic ocean thermohaline circulation: Nature, v. 393, no. 18, p. 673-676.

Hay, W., Soeding, E., DeConto, R., Wold, C., 2002, The late Cenozoic uplift – climate change paradox: International Journal of Earth Sciences, v. 91, no. 5, p. 746-774.

Irfan, T.Y., 1999, Characterization of weathered volcanic rocks in Hong Kong: Quaternary Journal of Engineering Geology, v. 32, p. 317-348.

Jafarzadeh, A.A., Burnham, C.P., 1992, Gypsum crystals in soils: Journal of Soil Science, v. 43, p. 409-420.

Kött, A., Gaupp, R., Wörner, G., 1995, Miocene to Recent history of the western Altiplano in northern Chile revealed by lacustrine sediments of the Lauca Basin (18°15’ - 18°40’S/69°30’ - 69°05’W): Geologische Rundschau, v. 84, no. 4, p. 770-780.

Martel, A.T., Gibling, M.R.., 2009, Wave-dominated lacustrine facies and tectonically controlled cyclicity in the Lower Carboniferous Horton Bluff Formation, Nova Scotia, Canada: Lacustrine Facies Analysis, p. 223-244.

Mees, F., 1999b, Textural features of Holocene perennial saline lake deposits of the Taudenni-Agorgott basin, northern Mali: Sedimentary Geology, v. 127, p. 65-84.

Mees, F., Castenda, C., Herrero, J., Ranst, E.V., 2012, The nature and significance of variations in gypsum crystal morphology in dry lake basins: Journal of Sedimentary Research, v. 82, p. 37-52.

Mercer, J.H., 1984, Late Cainozoic glacier variations in South America south of the Equator: Late Cainozoic Palaeoclimate of the Southern Hemisphere, SASQUA Symposium, Swaziland, p. 45-58.

Meyers, P.A., Ishiwatari, R., 1993, Lacustrine organic geochemistry – an overview of indicators of organic matter sources and diagenesis in lake sediments: Organic Geochemistry, v. 20, i. 7, p. 867-900.

Miller, K., Kominz, M., Browning, J., Wright, J., Mountain, G., Katz, M., Sugarman, P., Cramer, B., Christie-Blick, N., Pekar, S., 2005, The Phanerozoic record of global sea-level change: Science, v. 310, no. 1293, p. 1293-1298.

Montes, C., Cardona, A., Jaramillo, C., Pardo, A., Silva, J. C., Valencia, V., Ayala, C., Perez-Angel, L.C., Rodriguez-Parra, L. A., Ramirez, V., Nino, H., 2015, Middle Miocene closure of the Central American Seaway: Science, v. 348, no. 6231, p. 226-229.

Moon, C.F., Hurst, C.W., 1984, Fabric of muds and shales: an overview: Geological Society, London, Special Publications, v. 15, p. 579-593.

Mortimer, C., 1980, Drainage evolution in the Atacama Desert of northernmost Chile.

Mpodozis, C., Arriagada, C., Basso, M., Roperch, P., Cobbold, P., Reich, M., 2005, Late Mesozoic to Paleogene stratigraphy of the Salar de Atacama Basin, Antofagasta, northern Chile: implications for the tectonic evolution of the Central Andes: Tectonophysics, v. 399, i. 1-4, p. 125-154.

Munsell Color (Firm). Munsell Soil Color Charts: with genuine Munsell color chips. Grand Rapids, MI: Munsell Color, 2010.

O'Dea, A., Lessios, H., Coates, A., Eytan, R., Restrepo-Moreno, S., Cione, A., Collins, L., Queiroz, A., Farris, D., Norris, R., Stallard, R., Woodburne, M., Aguilera, O., Aubry, M., Berggren, W., Budd, A., Cozzuol, M., Coppard, S., Duque-Caro, H., Finnegan, S., Gasparini, G., Grossman, E., Johnson, K., Keigwin, L., Knowlton, N., Leigh, E., Leonard-Pingel, J., Marko, P., Pyenson, N., Rachello-Dolmen, P., Soibelzon, E., Soibelzon, L., Todd, J., Vermeij, G., Jackson, J., 2016, Formation of the Isthmus of Panama: Science Advances, v. 2, no. 8.

Orti, F., Rosell, L., Anadon, P., 2003, Deep to shallow lacustrine evaporates in the Libros gypsum (southern Teruel Basin, Miocene, ne Spain): an occurrence of pelletal gypsum rhythmites: Sedimentology, v. 50, p. 361-386.

Orti, F., Rosell, L., Ingles, M., 1997, Chert in continental evaporates of the Ebro and Calatayud basins (Spain): distribution and significance: Siliceous Rocks and Culture, v. 4, p. 75-89.

Parrish, J.T., Curtis, 1982, Atmospheric circulation, upwelling and organic-rich in the Mesozoic and Cenozoic eras: Paleogeography, Paleoclimatology, Paleoecology, v. 40, p. 31-66.

Parrish, J.T., Ziegler, A.M., Scotese, C.R., 1982, Rainfall patterns and the distribution of coals and evaporites in the Mesozoic and Cenozoic: Paleogeography, Paleoclimatology, Paleoecology, v. 40, p. 67-101.

Perez, A., Luzon, A., Roc, A.C., Soria, A.R., Mayayo, M.J., Sanchez, J.A., 2002, Sedimentary facies distribution and genesis of a recent carbonate-rich saline lake: Gallocanta Lake, Iberian Chain, NE Spain: Sedimentary Geology, v. 148, p. 185-202.

Placzek, C., Quade, J., Rech, J.A., Patchett, P.J., Perez de Arce, C., 2009, Geochemistry, chronology and stratigraphy of Neogene tuffs of the Central Andean region: Quaternary Geology, v. 4, p. 22-36.

Popp, B.N., Wilkinson, B.H., 1983, Holocene lacustrine ooids from Pyramid Lake, Nevada: Coated Grains, p. 142-153.

Quang, C.X., Clark, A.H., Lee, J.K.W., Hawkes, N., 2005, Response of supergene processes to episodic Cenozoic uplift, pediment erosion, and ignimbrite eruption in the Porphyry Copper Province of Southern Peru: Economic Geology, v. 100, i. 1, p. 87-114.

Rech, J., Currie, B., Michalski, G., Cowan, A., 2006, Neogene climate change and uplift in the Atacama Desert, Chile: Geology, v. 34, no. 9, p. 761-764.

Reijers, T.J.A., ten Have, A.H.M., 1983, Ooid zonation as indication for environmental conditions in a Givetian-Frasnian carbonate shelf-slope transition: Coated Grains, p. 188-198.

Richter, D.K., 1983, Calcareous ooids: a synopsis: Coated Grains, p. 71-99.

Rosen, M.R., Warren, J.K., 1990, The origin and significance of groundwater-seepage gypsum from Bristol Dry Lake, California, USA: Sedimentology, v. 37, p. 983-996.

Saez, A., Cabrera, L., Jensen, A., Chong, G., 1999, Late Neogene lacustrine record and paleogeography in the Quillagua-Llamara basin, Central Andean fore-arc (northern Chile): Paleogeography, Paleoclimatology, Paleoecology, v. 151, p. 5-37.

Schnurrenberger, D., Russell, J., Kelts, K., 2003, Classification of lacustrine sediments based on sedimentary components: Journal of Paleolimnology, v. 29, p. 141-154.

Schreiber, B.C., Tabakh, M.E., 2000, Deposition and early alteration of evaporites: Sedimentology, v 47, s. 1, p. 215-238.

Schroder, S., Schreiber, B.C., Amthor, J.E., Matter, A., 2003, A depositional model for the terminal Neoproterozoic-early Cambrian Ara Group evaporites in south Oman: Sedimentology, v. 50, p. 879-898.

Schroder, W., Worner, G., 1995, Miocene-Pleistocene ignimbrites in N-Chile, W-Bolivia and S-Peru: EGU Meeting, Strasbourg, Terra Abstr., Terra Nova, v. 7, p. 156.

Schroder, W., Worner, G., 1996, Widespread Cenozoic ignimbrites in N-Chile, W-Bolivia and S-Peru (17˚-20˚S/71˚-68˚E): stratigraphy, extension, correlation and origin: ISAG96 Andean Geodynamics extended abstracts, ORSTOM Collection Colloques et Seminaires, Paris, p. 465-468.

Smith, G.L.B., 1980, Logical-letter coding system for facies nomenclature: Witbank Coalfield: Transactions of the Geological Society of South Africa, v. 83, p. 301-311.

Stow, D.A.V., 2005, Sedimentary Rocks in the Field: a Color Guide.

Sturm, M., Matter, A., 1978, Turbidites and varves in Lake Brienz (Switzerland): deposition of clastic detritus by density currents: Modern and Ancient Lake Sediments, v. 2, p. 147-148.

Tucker, M.E., Wright, V.P., 2009, Carbonate depositional systems I: marine shallow-water and lacustrine carbonates: Carbonate Sedimentology, ch. 4.

Verges, J., Fernandez, M., Martinez, A., 2002, The Pyrenean orogeny: pre-, syn-, and post-collisional evolution: Journal of the Virtual Explorer, v. 8, p. 57-76.

Wara, M.W., Ravelo, A.C., Delaney, M.L., 2005, Permanent El Nino-like conditions during the Pliocene warm period: Science, v. 309, p. 758-761.

Warren, J.K., 2006, Evaporites: sediments, resources and hydrocarbons.

Warren, J.K., 2010, Evaporites through time: tectonic, climatic and eustatic controls in marine and nonmarine deposits: Earth-Science Reviews, v. 98, i. 3-4, p. 217-268.

Williams, M., Siveter, D.J., Ashworth, A.C., Wilby, P.R., Horne, D.J., Lewis, A.R., Marchant, D.R., 2008, Exceptionally preserved lacustrine ostracods from the middle Miocene of Antarctica: implications for high-latitude palaeoenviornment at 77 degrees south: Proceedings Biological Sciences, v. 275, i. 1650, p. 2449-2454.

Wörner, G., Hammerschmidt, K., Henjes-Kunst, F., Lezaun, J., Wilke, H., 2000, Geochronology ($^{40}Ar/^{39}Ar$, K-Ar and He-exposure ages) of Cenozoic magmatic rocks from Northern Chile (18-22˚S): implications for magmatism and tectonic evolution of the central Andes: Revista Geológica de Chile, v. 27, no. 2.

Wörner, G., Uhlig, D., Kohler, I., Seyfried, H., 2002, Evolution of the West Andean Escarpment at 18˚S (N. Chile) during the last 25 Ma: uplift, erosion and collapse through time: Tectonophysics, v. 345, i. 1-4, p. 183-198.

Zachos, J., Pagani, M., Sloan, L., Thomas, E., Billups, K., 2001, Trends, rhythms, and aberrations in global climate 65 Ma to present: Science, v. 292, no. 5517, p. 686-693.

Zaprowski, B.J., Pazzaglia, F.J., Evenson, E.B., 2005, Climatic influences on profile concavity and river incision: Journal of Geophysical Research, v. 110, i. F3.

Zhisheng, A., Kutzbach, J.E., Prell, W.L., Porter, S.C., 2001, Evolution of Asian monsoons and phased uplift of the Himalaya-Tibetan plateau since Late Miocene times: Nature, v. 411, no. 6833, p. 62-66.

APPENDIX A: SAMPLE DESCRIPTIONS

Sample	Elevation (m above river)	Lithofacies	Color (dry) - Munsell	Color (dry) - Description	Color (wet) - Munsell	Color (wet) - Description	Reaction w/ 10% HCL	Lithology	Stratigraphy	Other sedimentary features
LB 41	31.00	I	10y 8/1 (clay)	Light greenish gray (clay)	10y 7/1 (clay)	Light greenish gray (clay)	Calcareous - strongly calcareous	Clay	Slight very thin planar parallel laminae	Some black mottling
LB 40	22.50	V*	10yr 7/8, 5y 8/3 (sand)	Yellow, pale yellow (sand)	10yr 6/8, 5y 7/3	Brownish yellow, pale yellow (sand)	Not Calcareous	Sand	Convoluted wavy and non parallel laminae	Stain - 2.5y 7/6, 10yr 6/8
LB 39	21.80	III	10y 7/1 (sand), 5y 8/2 (clay)	Light greenish gray (sand), pale yellow (clay)	10y 6/1 (sand), 5y 7/2 (clay)	Greenish gray (sand), light gray (clay)	Strongly calcareous	Very fine sand, clay	Very thin planar parallel laminae	Stain - 10yr 6/8, 5yr 5/4, some black mottling
LB 38	21.00	II	10yr 7/8, 5y 8/3 (sand)	Yellow, pale yellow (sand)	10yr 6/8, 5y 7/3	Brownish yellow, pale yellow (sand)	Not Calcareous	Silty, ash		Stain - 2.5y 7/6, 10yr 6/8
LB 37	20.20	I	10y 8/1	Light greenish gray	10y 7/1 (clay)	Light greenish gray	Not Calcareous	Clay	Slight very thin planar parallel laminae	Stain - 2.5y 7/6, some black mottling
LB 36	19.40	II	5gy 6/1	Greenish gray	5gy 5/1	Greenish gray	Not Calcareous	Silty, ash		
LB 35	18.40	I*	10y 7/1 (sand), 10y 8/1 (clay)	Light greenish gray (both)	10y 6/1 (sand), 10y 7/1 (clay)	Greenish gray (sand), light greenish gray (clay)	Calcareous - strongly calcareous	Very fine sand, clay	Medium planar parallel laminae	Some black mottling
LB 34	17.40	V*	10yr 7/3	Very pale brown	10yr 6/3	Pale brown	Not - slightly calcareous	Very fine sand	Fine planar parallel laminae	Stain - 10yr 6/8

LB 33	16.90	III	10y 7/1 (sand), 10y 8/1 (clay), 5gy 7/1 (clay)	Light greenish gray (all)	10y 6/1 (sand), 10y 7/1 (clay), 5gy 6/1	Greenish gray (sand), light greenish gray (clay), greenish gray (clay)	Calcareous - strongly calcareous	Very fine sand, clay	Medium planar parallel laminae	Stain - 7.5yr 5/8, 7.5yr 7/6, some black mottling
LB 32	15.40	III	10y 7/1 (sand), 10y 8/1 (clay)	Light greenish gray (both)	10y 6/1 (sand), 10y 7/1 (clay)	Greenish gray (sand), light greenish gray (clay)	Calcareous - strongly calcareous	Very fine sand, clay	Medium planar parallel laminae	Stain - 7.5yr 5/8, 7.5yr 7/6, 7.5yr 4/4
LB 31	14.40	III*	5yr 7/3, 10y 7/1 (sand)	Pink, light gray	5yr 6/3, 10y 6/1 (sand)	Light reddish brown, greenish gray (sand)	Strongly calcareous	Sand	Fine - medium convoluted wavy and non parallel laminae	Stain - 10yr 6/8, some black mottling
LB 30	14.00	I*	10y 7/1 (sand), 10y 8/1 (clay), 5gy 7/1 (clay)	Light greenish gray (all)	10y 6/1 (sand), 10y 7/1 (clay), 5gy 6/1	Greenish gray (sand), light greenish gray (clay), greenish gray (clay)	Not Calcareous - slightly calcareous	Very fine sand, clay	Medium planar parallel laminae	Stain - 7.5yr 5/8, 7.5yr 7/6, some black mottling
LB 29	13.40	I	5y 8/3	Pale yellow	5y 7/4	Pale yellow	Strongly calcareous	Clay		Stain - 7.5 yr 7/4 (pink), some black mottling
LB 28	11.20	III	10y 7/1 (sand), 10y 8/1 (clay)	Light greenish gray (both)	10y 6/1 (sand), 10y 7/1 (clay)	Greenish gray (sand), light greenish gray (clay)	Strongly calcareous	Sand, clay	Medium planar parallel laminae	
LB 27	9.20	I	10y 8/1	Light greenish gray	10y 7/1	Light greenish gray	Calcareous	Very fine sand, clay	Very thin planar parallel laminae	Some black mottling
LB 26	8.40	IV*	10y 7/1 (sand), 10y 8/1 (clay)	Light greenish gray (both)	10y 6/1 (sand), 10y 7/1 (clay)	Greenish gray (sand), light greenish gray (clay)	Calcareous - strongly calcareous	Very fine sand, clay	Fine - medium planar parallel laminae, slightly convoluted/disturbed	Stain - 5yr 5/8 (yellowish red), 7.5yr 6/8 (reddish yellow), some black mottling

LB 9	5.70	III	5y 7/3 (sand), 5y 8/2 (clay)	Pale yellow (both)	2.5y 5/4 (sand), 5y 7/2 (clay)	Light olive brown (sand), light gray (clay)	Calcareous - strongly calcareous	Very fine-fine sand, clay	Fine - medium planar parallel laminae, slightly convoluted/disturbed	
LB 10	5.40	I	10y 7/1 (sand), 5y 8/2 (clay)	Light greenish gray (sand), pale yellow (clay)	10y 6/1 (sand), 5y 7/2 (clay)	Greenish gray (sand), light gray (clay)	Not - slightly calcareous	Very fine-fine sand, clay	Wavy and/or convoluted laminae	
LB 11	5.00	IV*	10y 7/1 (sand), 10y 8/1 (clay), 5y 8/2 (clay)	Light greenish gray (sand), light greenish gray (clay) , pale yellow (clay)	10y 6/1 (sand), 10y 7/1 (clay), 5y 7/3 (clay)	Greenish gray (sand), light greenish gray (clay) , pale yellow (clay)	Slightly calcareous	Sand, clay	Convoluted wavy and non parallel laminae	Stain - 2.5y 7/6
LB 12	4.60	III	10y 7/1 (sand), 10y 8/1 (clay), 5y 8/2 (clay)	Light greenish gray (sand), light greenish gray (clay) , pale yellow (clay)	10y 6/1 (sand), 10y 7/1 (clay), 5y 7/3 (clay)	Greenish gray (sand), light greenish gray (clay), pale yellow (clay)	Strongly calcareous	Sand, clay	Convoluted wavy and non parallel laminae	Stain - 2.5y 7/6
LB 13	4.45	IV*	10y 5/1 (gypsum) , 10y 7/1 (sand), 10y 8/1 (clay)	Greenish gray (gypsum), light greenish gray (sand), light greenish gray (clay)	10y 4/1 (gypsum) , 10y 6/1 (sand), 10y 7/1 (clay)	Dark greenish gray (gypsum), greenish gray (sand), light greenish gray (clay)	Slightly - calcareous	Gypsum, sand, clay	Convoluted wavy and non parallel laminae	Gypsum crystals, stain - 10yr 4/4, 10yr 7/6, 10yr 6/6

LB 14	4.35	III	10y 7/1 (sand), 10y 8/1 (clay)	Light greenish gray (both)	10y 6/1 (sand), 10y 7/1 (clay)	Greenish gray (sand), light greenish gray (clay)	Strongly calcareous	Very fine sand, clay	Very thin wavy and non parallel laminae, localized lenticular lamination	Stain - 2.5y 7/6
LB 15	4.00	III	10y 8/1 (clay)	Light greenish gray	10y 7/1 (clay)	Light greenish gray	Strongly calcareous	Clay		Stain - 2.5y 7/6, some black mottling
LB 16	3.95	IV	10y 5/1 (gypsum), 10y 8/1 (clay)	Greenish gray (gypsum), light greenish gray (clay)	10y 4/1 (gypsum), 10y 7/1 (clay)	Dark greenish gray (gypsum), light greenish gray (clay)	Not - slightly calcareous	Gypsum, clay		Gypsum crystals, stain - 5yr 6/8, 5yr 5/8
LB 17	3.80	V	10y 8/1	Light greenish gray	10y 7/1	Light greenish gray	Slightly calcareous	Sand	Possible wavy and non parallel laminae	
LB 6	3.10	III	10y 7/1 (sand), 10y 8/1 (clay)	Light greenish gray (both)	10y 6/1 (sand), 10y 7/1 (clay)	Greenish gray (sand), light greenish gray (clay)	Strongly calcareous	Very fine sand, clay	Very fine to medium wavy and non parallel laminae	Stains - 5yr 8/6 (reddish yellow)
LB 18	3.00	IV*	10y 7/1 (sand), 10y 8/1 (clay)	Light greenish gray (both)	5gy 6/1 (sand), 10y 7/1 (clay)	Greenish gray (sand), light greenish gray (clay)	Strongly calcareous	Very fine sand, clay	Convoluted wavy and non parallel laminae very fine to medium	Stains - 10yr 4/6 (dark yellowish brown), 10yr 5/8 (yellowish brown)
LB 25	2.55	I	10y 7/1 (sand), 10y 8/1 (clay)	Light greenish gray (both)	5gy 6/1 (sand), 10y 7/1 (clay)	Greenish gray (sand), light greenish gray (clay)	Calcareous	Very fine sand, clay		Stains - 10yr 5/6 (yellowish brown), 10yr 7/6 (yellow)
LB 24	2.43	I	10y 7/1 (sand), 10y 8/1 (clay)	Light greenish gray (both)	5gy 6/1 (sand), 10y 7/1 (clay)	Greenish gray (sand), light greenish gray (clay)	Slightly calcareous	Very fine sand, clay	Very fine planar parallel laminae	Stains - 5yr 6/6 (reddish yellow)

LB 23	2.25	II	10y 6/1-10y 7/1	Greenish gray - light greenish gray	10y 5/1-10y 6/1	Greenish gray (both)	Not Calcareous	Silty, ash		
LB 4	2.00	II*	10y 6/1 (sand), 10y 8/1 (clay)	Greenish gray (sand), light greenish gray (clay)	10y 5/1 (sand), 10y 7/1 (clay)	Greenish gray (sand), light greenish gray (clay)	Slightly calcareous	Very fine-fine sand, clay	Possible graded planar parallel to slightly wavy and non parallel localized lenticular lamination of sand without cross laminations	Possible current pushed ripples
LB 22	1.91	III	10y 8/1	Light greenish gray	10y 7/1	Light greenish gray	Strongly calcareous	Clay	Very thin planar parallel laminae	
LB 21	1.83	I*	10y 7/1 (sand), 10y 8/1 (clay)	Light greenish gray (both)	5gy 6/1 (sand), 10y 5/1 (clay)	Greenish gray (both)	Not - slightly calcareous	Very fine sand, clay	Thin (1-3mm) alternating laminae	
LB 5	1.68	V	5y 8/2	Pale yellow	10yg 6/1	Greenish gray	Not Calcareous	Coarse sand		Stains - 10yr 6/6 (brownish yellow)
LB 19	1.66	I	10y 7/1	Light greenish gray	10y 5/1	Greenish gray	Calcareous	Clay	Very thin to medium planar parallel laminae	Very few laminae - N 8/0 (white)
LB 20	1.28	I*	10y 8/1	Light greenish gray	10y 6/1	Greenish gray	Not - slightly calcareous	Clay	Very thin planar parallel laminae	Stains or mottles (oxidation of sulfides?) - 5y 8/6 (yellow), 10yr 7/8 (yellow)

*: denotes sample lithofacies was confirmed via petrographic analysis

APPENDIX B: PETROGRAPHIC DESCRIPTIONS

Thin Section: LB20

Lithology: Laminated mudstone, non-calcareous

Sediment Grains: Overall: approximately 60% clay matrix, 10% muddy silt matrix, 20% siliciclastic grains (0.05-0.1 mm in diameter), 5% gypsum crystals (0.05-0.2 mm in diameter), and 5% volcanic fragments (0.05-0.4 mm diameter). Common mica (biotite) grains (0.05-0.1 mm in diameter) throughout exhibit oxidation of Fe^{2+} to Fe^{3+}, very few plagioclase grains (0.15 mm in diameter) and very few olivine grains (0.05-0.075 mm in diameter) present. Sediment grains are overall subhedral to anhedral, undulating to smooth, and sub-rounded to rounded.

Authigenic Minerals: Few clusters of euhedral gypsum crystals (0.05-0.2 mm in diameter). Most of the gypsum crystals in the thin section are partially to fully replaced by chalcedony and have anhedral to subhedral, sublenticular to lenticular forms. Many gypsum crystals appear to have been plucked during the preparation of the thin section.

Sedimentary Fabric: Discontinuous, irregular, and very thin (0.005-0.03 mm) laminae. Individual laminae consist chiefly of clay, but there are few sandy and silty laminae, and very few elongate lenses of micritic carbonate and sand matrix (0.5-1.0 mm diameter parallel to bedding) present. Clay laminae display unistrial birefringence and appear light yellow to yellow in cross-polarized light.

Biogenic Structures: Few carbonate peloids (0.01-0.02 mm in diameter) and possible filled burrows (0.075 mm diameter parallel to bedding), or very small, elongate lenses of micritic carbonate.

Organic Material: Small, opaque grains (approximately 0.001 mm in diameter) may be organic matter or pyrite fragments.

Notes: Reddish staining present throughout. Most of the staining forms long, thick streaks (0.5-1.0 mm in diameter), while other manifestations appear in clustered fragments that may represent oxidized crystals of a primary mineral (0.025-0.05 mm diameter). Black staining can be seen throughout as very thin, undulating lines (0.001-0.025 mm diameter parallel to bedding).

Thin Section: LB21

Lithology: Laminated mudstone, noncalcareous

Sediment Grains: Overall: approximately 60% clay matrix, 10% muddy silt matrix, 15% siliciclastic grains (0.05-0.1 mm in diameter), 5% gypsum crystals (0.05-0.2 mm in diameter), 5% volcanic fragments (0.05-0.4 mm diameter), and 5% siliciclastic sediment pellets and carbonate peloids (0.1-0.25 mm in diameter) that appear to have been compacted together. Common mica (biotite) grains (0.05-0.1 mm in diameter) throughout exhibit oxidation of Fe^{2+} to Fe^{3+}, very few plagioclase grains (0.15 mm in diameter), and very few olivine grains (0.05-0.075 mm in diameter). Sediment grains are overall subhedral to anhedral, undulating to smooth, and sub-rounded to rounded.

Authigenic Minerals: Few clusters of euhedral gypsum crystals (0.05-0.2 mm in diameter), some appear sub-rounded. Most gypsum crystals are partially to fully replaced by chalcedony and many appear to have anhedral to subhedral and lenticular to sublenticular forms. Many gypsum crystals appear to have been plucked during the preparation of the thin section.

Sedimentary Fabric: Discontinuous, irregular, and very thin (0.005-0.5 mm) laminae. Individual laminae consist chiefly of clay, but few sandy and silty laminae, and very few elongate lenses of micritic carbonate and sand (0.5-1.0 mm diameter parallel to bedding) are additionally present. Clay laminae display unistrial birefringence and appear light yellow to yellow in cross-polarized light.

Biogenic Structures: Carbonate peloids (0.01-0.02 mm in diameter) and possible filled burrows (0.075 mm diameter parallel to bedding), or very small elongate lenses of micritic carbonate. Very few calcareous fossil fragments throughout; some resemble ostracodes (0.05-0.25 mm in diameter).

Organic Material: Small, opaque grains (approximately 0.001 mm in diameter) may be organic matter or pyrite fragments.

Notes: Reddish staining throughout. Most of the staining forms long, thick streaks (0.5-1.0 mm in diameter), while other manifestations appear in clustered fragments that may represent oxidized crystals of a primary mineral (0.025-0.05 mm diameter). Black staining can be seen throughout as very thin, undulating lines (0.001-0.025 mm diameter parallel to bedding).

Thin Section: LB4

Lithology: Volcaniclastic mudrock: ashy siltstone, ashy mudstone, ashy claystone, silty ash

Sediment Grains: Overall: approximately 60% volcanic fragments (0.05-0.4 mm diameter), 20% muddy, silt, or clay matrix depending on the dominant microfacies, 15% siliciclastic grains (0.05-0.1 mm diameter), and 5% gypsum crystals (0.05-0.1 mm diameter). Plagioclase grains (0.15-0.3 mm diameter), mica (biotite) grains (0.05-0.1 mm

diameter), and olivine grains (0.05-0.1 mm diameter) are dominant in ashy siltstone and silty ash laminae. Sediment grains are overall subhedral (few to frequent euhedral grains are present), undulating to smooth, and subangular.

Authigenic Minerals: Few, subhedral, lenticular gypsum crystals (0.05-0.1 mm diameter). Some gypsum crystals are partially to fully replaced by chalcedony and many appear to have anhedral to subhedral and lenticular to sublenticular forms.

Sedimentary Fabric: Laminae are discontinuous, irregular, and vary in thickness (0.05-0.5 mm diameter parallel to bedding). Individual laminae consist chiefly of volcaniclastic sediment; however, clayey, silty, and ash-rich laminae are common. Volcaniclastic laminae (2.0-2.5 mm diameter parallel to bedding) are dominantly present in ashy siltstone, ashy claystone, silty ash microfacies.

Biogenic Structures: None.

Organic Material: Small, opaque grains (approximately 0.001 mm in diameter) may be organic matter or pyrite fragments.

Notes: Reddish staining present throughout. Most of the staining forms long, thick streaks (0.5-1.0 mm diameter parallel to bedding), while other manifestations appear in clustered fragments that may represent oxidized crystals of a primary mineral (0.025-0.05 mm diameter). Domains with volcanic material display prominent staining.

Thin Section: LB18

Lithology: Evaporite: gypsum and carbonate

Sediment Grains: Overall: approximately 40% gypsum crystals (0.025-0.1 mm diameter), 25% micritic carbonate matrix, 20% clay matrix, 10% siliciclastic grains (0.01-0.5 mm diameter), and 5% carbonate peloids (0.01-0.02 mm diameter). The

sample consists of four distinct microfacies: (1) 80-100% evaporite crystals and 0-20% matrix, sub-horizontally aligned, subhedral lenticular, closely packed and interlocked, (2) 40-50% evaporite crystals and 50-60% matrix, randomly oriented and unaligned, elongate and lenticular with a dominantly micritic carbonate matrix, (3) 90-95% evaporite crystals and 5-10% matrix, randomly oriented and aligned, variably shaped, intergrown and interlocked, and (4) 90-100% evaporite crystals and 0-10% matrix, randomly oriented and aligned, equant tabular prismatic, and intergrown. Common mica (biotite) grains (0.05-0.1 mm diameter), and very few olivine grains (0.05-0.075 mm diameter). Sediment grains are overall subhedral (frequent euhedral grains are present), undulating to smooth, and subangular.

Authigenic Minerals: Subhedral, lenticular gypsum crystals (0.025-0.1 mm diameter) are dominant to very dominant.

Sedimentary Fabric: Laminae are discontinuous, irregular, and vary in thickness (0.05-3.0+ mm). Individual laminae consist chiefly of clay or gypsum (present variably in mixtures of gypsum and clay, and individual gypsum or clay laminae), although there are some laminae and elongate lenses of micritic carbonate (0.5-1.0 mm diameter parallel to bedding). Crude inverse grading from fine grained gypsum crystals in a micritic carbonate matrix upward into coarse gypsum crystals and clusters of intergrown crystals is apparent in some areas.

Biogenic Structures: Few carbonate peloids (0.01-0.02 mm diameter) surrounded and engulfed by gypsum crystals. Individual gypsum crystals have inclusions of micrite.

Organic Material: None.

Notes: Reddish staining present throughout. Most of the staining forms long, thick streaks (0.5-1 mm diameter parallel to bedding), while other manifestations appear in clustered fragments that may represent oxidized crystals of a primary mineral (0.025-0.05 mm diameter).

Thin Section: LB13

Lithology: Evaporite: gypsum and claystone

Sediment Grains: Overall: approximately 60% gypsum crystals (0.1-0.5 mm diameter), 30% silty and sandy clay matrix, and 10% siliciclastic grains (.003-.05 mm diameter). Common mica (biotite) grains (0.05-0.1 mm diameter) that exhibit oxidation of Fe^{2+} to Fe^{3+}, very few feldspar (plagioclase) grains (0.3 mm diameter), and very few olivine grains (0.05-0.075 mm diameter) present. Few plagioclase grains exhibit twinning and growth lines. Sediment grains are overall subhedral (frequent euhedral grains are present), undulating to smooth, and subangular.

Authigenic Minerals: Subhedral, lenticular gypsum crystals (0.1-0.5 mm diameter) are dominant to very dominant. Most of these gypsum clusters are either lenticular tabular prismatic or equant in form, and many are subhorizontally stacked with few randomly oriented zones. Many gypsum crystal clusters are dominantly engulfed and distributed throughout matrix, while many have are more dominantly concentrated together.

Sedimentary Fabric: Laminae are discontinuous, irregular, and vary in thickness (0.05-0.3 mm). Individual laminae consist chiefly of crude lenses of intergrown gypsum crystals (present variably in mixtures of gypsum and clay, and individual gypsum or clay laminae)(0.5-1.0 mm), laminae of lenticular gypsum crystals locally oriented subhorizontally to subvertically, and slightly silty clay. Crude inverse grading from fine

grained evaporite crystals in a micritic carbonate matrix to coarse and intergrown evaporite clusters present in some domains. Clay laminae display unistrial birefringence and appear light yellow-yellow in cross polarized light.

Biogenic Structures: None.

Organic Material: None.

Notes: Reddish staining present throughout. Most of the staining forms long, thick streaks (0.5-1 mm diameter parallel to bedding), while other manifestations appear in clustered fragments that may represent oxidized crystals of a primary mineral (0.025-0.05 mm diameter).

Thin Section: LB11

Lithology: Evaporite: gypsum and claystone

Sediment Grains: Overall: approximately 30% mud or silty clay matrix, 30% gypsum crystals (0.025-0.1 mm diameter), 20% micritic carbonate matrix, 15% monomineralic siliciclastic grains (.003-.05 mm diameter), and 5% volcanciclastic material (0.05-0.4 mm diameter). Common mica (biotite) grains (0.05-0.1 mm diameter) throughout exhibit oxidation of Fe^{2+} to Fe^{3+}, very few feldspar (plagioclase) grains (0.3 mm diameter), and very few hornblende grains (0.3 mm diameter). Sediment grains are overall subhedral (very few to few euhedral grains are present), undulating to smooth, and sub-rounded to subangular.

Authigenic Minerals: Clusters of intergrown euhedral to subhedral, lenticular tabular gypsum crystals (0.025-0.1 mm diameter) are dominant to very dominant (0.05-0.2 mm diameter), some appear sub-rounded. Most of these gypsum crystals are partially to fully replaced by chalcedony and many appear sub-rounded with anhedral-subhedral and

lenticular-sublenticular outlines. Many gypsum crystals appear to have been plucked during the preparation of the thin section.

Sedimentary Fabric: Laminae are discontinuous, irregular, and vary in thickness (0.05-0.3 mm). Individual laminae consist chiefly of clay and gypsum (present variably in mixtures of gypsum and clay, and individual gypsum or clay laminae); there are also very few micritic carbonate laminae.

Biogenic Structures: None.

Organic Material: None.

Notes: None.

Thin Section: LB26

Lithology: Evaporite: gypsum and claystone, gypsum and carbonate

Sediment Grains: Overall: approximately 35% gypsum crystals (0.05-0.5 mm diameter), 25% evaporite matrix, 15% clay matrix, 10% micritic carbonate matrix, 10% siliciclastic grains (0.01-0.5 mm diameter), and 5% carbonate ooids and peloids (0.01-0.02 mm diameter). Nevertheless, the sample consists of four distinct microfacies: (1) one consisting of 80-100% evaporite crystals, subhoriztonal, closely packed, subhedral, and interlocked; (2) one consisting of 40-50% evaporite crystals, randomly oriented, elongate and lenticular with a dominantly micritic carbonate matrix; (3) one consisting of 90-95% evaporite crystals, randomly oriented, intergrown and interlocked; and (4) one consisting of 90-100% evaporite crystals, randomly oriented, equant, tabular prismatic, acicular, and intergrown. Common mica (biotite) grains (0.05-0.1 mm diameter), and very few olivine grains (0.05-0.075 mm diameter). Sediment grains are overall subhedral to anhedral (very few euhedral grains are present), undulating to smooth, and sub-rounded. Sediment

grains are dominantly present within applicable microfacies laminae and are not distributed throughout.

Authigenic Minerals: Subhedral, lenticular tabular gypsum crystals (0.05-0.5 mm diameter) are dominant to very dominant. Most clusters of gypsum crystals are subhorizontally to horizontally stacked and they are, for the most part, intergrown.

Sedimentary Fabric: Very well-defined laminae of different microfacies distinctly alternate, and vary in thickness (0.05-3.0+ mm diameter). Individual laminae consist chiefly of stacked, subhorizontal gypsum crystals in a clay matrix. Microlaminae of varying gypsum crystal morphologies are present within clay laminae (0.025-0.075 mm diameter), and possible stylolites exist in gypsum laminae. Crude inverse grading from fine grained evaporite crystals in a micritic carbonate matrix to coarse and intergrown evaporite clusters present in some domains. Clay laminae display unistrial birefringence and appear light yellow-yellow in cross polarized light.

Biogenic Structures: Frequent carbonate ooids (0.01-0.02 mm diameter) and carbonate peloids (0.01-0.02 mm diameter). Few filled burrows or cross-sectioned filled burrows (0.2 mm diameter parallel to bedding); however the "burrows" might be elongate lenses of micritic carbonate. Fossil fragments and fossils of unknown origin are frequent throughout; some resemble ostracodes (0.05-0.25 mm in diameter).

Organic Material: Small, opaque grains (approximately 0.001 mm in diameter) may be organic matter or pyrite fragments.

Notes: Reddish staining present throughout. Most of the staining forms long, thick streaks (0.5-1 mm diameter parallel to bedding), while other manifestations appear in

clustered fragments that may represent oxidized crystals of a primary mineral (0.025-0.05 mm diameter).

Thin Section: LB30

Lithology: Laminated mudstone, calcareous

Sediment Grains: Overall: approximately 60% fine-grained clay matrix, 15% micritic carbonate matrix, 20% siliciclastic grains (0.05-0.2 mm diameter), and 5% gypsum crystals (0.05-0.2 mm in diameter). Common mica (biotite) grains (0.05-0.1 mm diameter) exhibit oxidation of Fe^{2+} to Fe^{3+}, very few feldspar (plagioclase) grains (0.1 mm diameter), and very few olivine grains (0.05-0.075 mm diameter) present. Sediment grains are overall subhedral (few to frequent euhedral grains are present), undulating to smooth, and sub-rounded to rounded.

Authigenic Minerals: Few, mainly euhedral, gypsum crystals (0.05-0.2 mm in diameter). Most of these gypsum crystals are partially-fully replaced by chalcedony and many appear sub-rounded with anhedral-subhedral and lenticular-sublenticular outlines.

Sedimentary Fabric: Laminae are discontinuous, irregular, and vary in thickness (0.05-4.0 mm diameter). Individual laminae consist chiefly of clay or micritic carbonate, with few, elongate lenses of micritic carbonate (0.5-1.0 mm diameter parallel to bedding) throughout. Crude inverse grading in clay laminae from clay to silty clay is present. Clay laminae display unistrial birefringence and appear light yellow-yellow in cross polarized light.

Biogenic Structures: Few carbonate peloids (0.01-0.02 mm diameter).

Organic Material: Possible silicified algal features (microbial mats), fragments of which are elongate and parallel to bedding and include silt grains. Small, opaque grains (approximately 0.001 mm in diameter) may be organic matter or pyrite fragments.

Notes: Reddish staining present throughout. Most of the staining forms long, thick streaks (0.5-1 mm diameter parallel to bedding), while other manifestations appear in clustered fragments that may represent oxidized crystals of a primary mineral (0.025-0.05 mm diameter). Black staining can be seen throughout as very thin, undulating lines (0.001-0.025 mm diameter parallel to bedding)

Thin Section: LB31

Lithology: Carbonate: sandy carbonate

Sediment Grains: Overall approximately: 60% micritic carbonate matrix, 15% clay matrix, 12.5% siliciclastic grains (0.03-0.2 mm diameter), 7.5% gypsum crystals (0.025-0.1 mm diameter), and 5% volcaniclastic material (0.1-0.4 mm diameter). Frequent mica (biotite) grains (0.05-0.1 mm diameter) throughout exhibit oxidation of Fe^{2+} to Fe^{3+}, very few plagioclase grains (0.1 mm diameter). Frequent voids (0.025-0.1 mm diameter) present throughout. Sediment grains are overall euhedral to subhedral, undulating to smooth, and subangular.

Authigenic Minerals: Common euhedral to subhedral, lenticular tabular gypsum crystals (0.025-0.1 mm diameter). Most of these gypsum crystals are partially to fully replaced by chalcedony and many appear sub-rounded, with anhedral to subhedral, and sublenticular to lenticular outlines. Many gypsum crystals appear to have been plucked during the preparation of the thin section.

Sedimentary Fabric: Somewhat continuous laminae near the top of the thin section, with no other obvious laminae throughout. Very few elongate lenses of micritic carbonate (0.5-1.0 mm diameter parallel to bedding). Many of the carbonate laminae appear to exhibit signs of autobrecciation or nodularization, and voids are filled with crystalline calcite.

Biogenic Structures: Carbonate peloids (0.01-0.02 mm diameter) common throughout. Ostracodes and other calcareous fossil fragments are common throughout (0.05-0.25 mm in diameter).

Organic Material: Small, opaque grains (approximately 0.001 mm in diameter) may be organic matter or pyrite fragments.

Notes: Reddish staining present throughout. Most of the staining forms long, thick streaks (0.5-1 mm diameter parallel to bedding), while other manifestations appear in clustered fragments that may represent oxidized crystals of a primary mineral (0.025-0.05 mm diameter). Autobrecciation and nodularization indicate subaerial exposure. Oxidized pyrite framboids are possible in some domains.

Thin Section: LB34

Lithology: Muddy sandstone, laminated (some locally massive zones)

Sediment Grains: Overall: approximately 70% siliciclastic grains (0.05-0.2 mm diameter), 10% fine-grained muddy matrix, 12.5% volcaniclastic grains (0.1-0.4 mm diameter), 5% gypsum crystals (0.025-0.1 mm diameter), and 2.5% micritic carbonate matrix. Approximately 50% of the volcaniclastic material consists of volcanic glass fragments. Common mica (biotite) grains (0.05-0.1 mm diameter) that exhibit oxidation of Fe^{2+} to Fe^{3+}, very few feldspar (plagioclase) grains (0.1 mm diameter), very few

olivine crystals (0.05-0.1 mm diameter), very few augite grains (0.15-0.3 mm diameter), and very few sanidine grains present. Sediment grains are overall euhedral to subhedral, undulating to smooth, and subangular.

Authigenic Minerals: Few, euhedral, lenticular tabular gypsum crystals (0.025-0.1 mm diameter). Most gypsum crystals are partially to fully replaced by chalcedony and many appear sub-rounded with anhedral-subhedral and lenticular-sublenticular outlines.

Sedimentary Fabric: Vague laminae are discontinuous, irregular, and vary in thickness (0.025-0.2 mm diameter parallel to bedding), and some domains of the thin section exhibit massive fabric. Individual laminae consist chiefly of coarse grains and mica that are subhorizontal to horizontally oriented. Very few elongate lenses of micritic carbonate (0.5-1.0 mm diameter parallel to bedding).

Biogenic Structures: Possible filled burrows (0.1 mm diameter parallel to bedding) present, however the "burrows" might be elongate lenses of micritic carbonate.

Organic Material: None.

Notes: Reddish staining present throughout. Most of the staining forms long, thick streaks (0.5-1 mm diameter parallel to bedding), while other manifestations appear in clustered fragments that may represent oxidized crystals of a primary mineral (0.025-0.05 mm diameter). Black staining can be seen throughout as very thin, undulating lines (0.001-0.025 mm diameter parallel to bedding).

Thin Section: LB35

Lithology: Laminated mudstone: calcareous

Sediment Grains: Overall: approximately 20-40% micritic carbonate matrix, 20-40% finely ground clay matrix, 15% muddy peloids (0.01-0.02 mm diameter) and carbonate

peloids (0.01-0.02 mm diameter), 10% subhedral aggregates of carbonate (0.01-0.02 mm diameter), 10% siliciclastic grains (0.05-0.15 mm diameter), and 5% gypsum crystals (0.025-0.1 mm diameter). Common mica (biotite) grains (0.05-0.1 mm diameter) throughout exhibit oxidation of Fe^{2+} to Fe^{3+}, few feldspar (plagioclase) grains (0.15 mm diameter), and very few olivine grains (0.05-0.1 mm diameter). The subhedral aggregates of carbonate appear to be similar in size and shape to the carbonate peloids present but are distinct from them in that they are not strictly rounded and appear compressed in some cases. They also appear to be shaped more similarly to sediment grains than peloids in most cases. Sediment grains are overall subhedral (very few euhedral grains are present), undulating to smooth, and rounded to sub-rounded.

Authigenic Minerals: Few, euhedral, lenticular tabular gypsum crystals (0.025-0.1 mm diameter). Most of these gypsum crystals are partially-fully replaced by chalcedony and many of them appear sub-rounded with anhedral-subhedral and lenticular-sublenticular outlines.

Sedimentary Fabric: Vague laminae are discontinuous, irregular, and vary in thickness (0.025-0.2 mm diameter). Individual laminae consist chiefly of clay or micritic carbonate; however, few laminae of muddy peloids and carbonate peloids are additionally present. Thin strings of clastic material (0.1-0.2 mm diameter) frequent.

Biogenic Structures: Carbonate peloids (0.01-0.02 mm diameter) present throughout. Possible fossils and fossil fragments of unknown origin are frequent throughout (0.05-0.25 mm in diameter).

Organic Material: None.

Notes: Reddish staining present throughout. Most of the staining forms long, thick streaks (0.5-1 mm diameter parallel to bedding), while other manifestations appear in clustered fragments that may represent oxidized crystals of a primary mineral (0.025-0.05 mm diameter). Black staining can be seen throughout as very thin, undulating lines (0.001-0.025 mm diameter parallel to bedding).

Thin Section: LB40

Lithology: Muddy sandstone: massive

Sediment Grains: Overall: approximately 50% mud matrix, 40% siliciclastic clay- to sand-sized grains (0.025-0.2 mm diameter), 5% gypsum crystals (0.025-0.1 mm diameter), and 5% volcaniclastic material (0.05-0.4 mm diameter). Dominant mica (biotite) grains (0.05-0.1 mm diameter) throughout exhibit oxidation of Fe^{2+} to Fe^{3+}, and have a "birds eye maple" appearance, frequent feldspar (plagioclase) grains (0.15 mm diameter), few olivine grains (0.05-0.1 mm diameter), few augite grains (0.15-0.3 mm diameter), and few sanidine grains (0.15-0.3 mm diameter) are present. Sediment grains are overall euhedral to subhedral, undulating to smooth, and sub-rounded to subangular.

Authigenic Minerals: Few euhedral, lenticular tabular gypsum crystals (0.025-0.1 mm diameter).

Sedimentary Fabric: Massive fabric with no obvious laminae.

Biogenic Structures: None.

Organic Material: None.

Notes: Reddish staining present throughout. Some of the staining forms long, thick streaks (0.5-1 mm diameter parallel to bedding), while other manifestations appear in

clustered fragments that may represent oxidized crystals of a primary mineral (0.025-0.05 mm diameter).

APPENDIX C: PHOTOMICROGRAPHS OF THIN SECTIONS

LB4

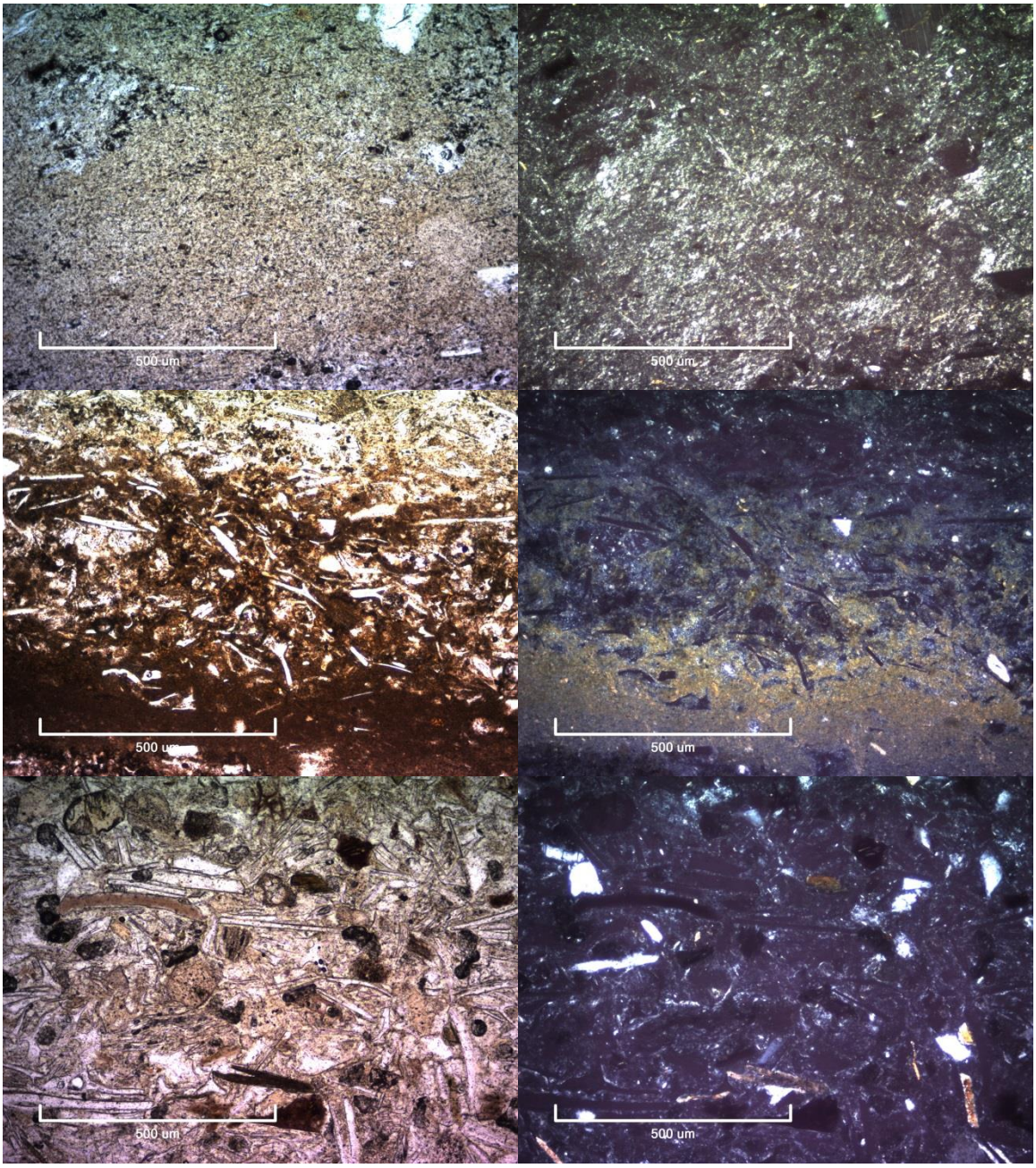

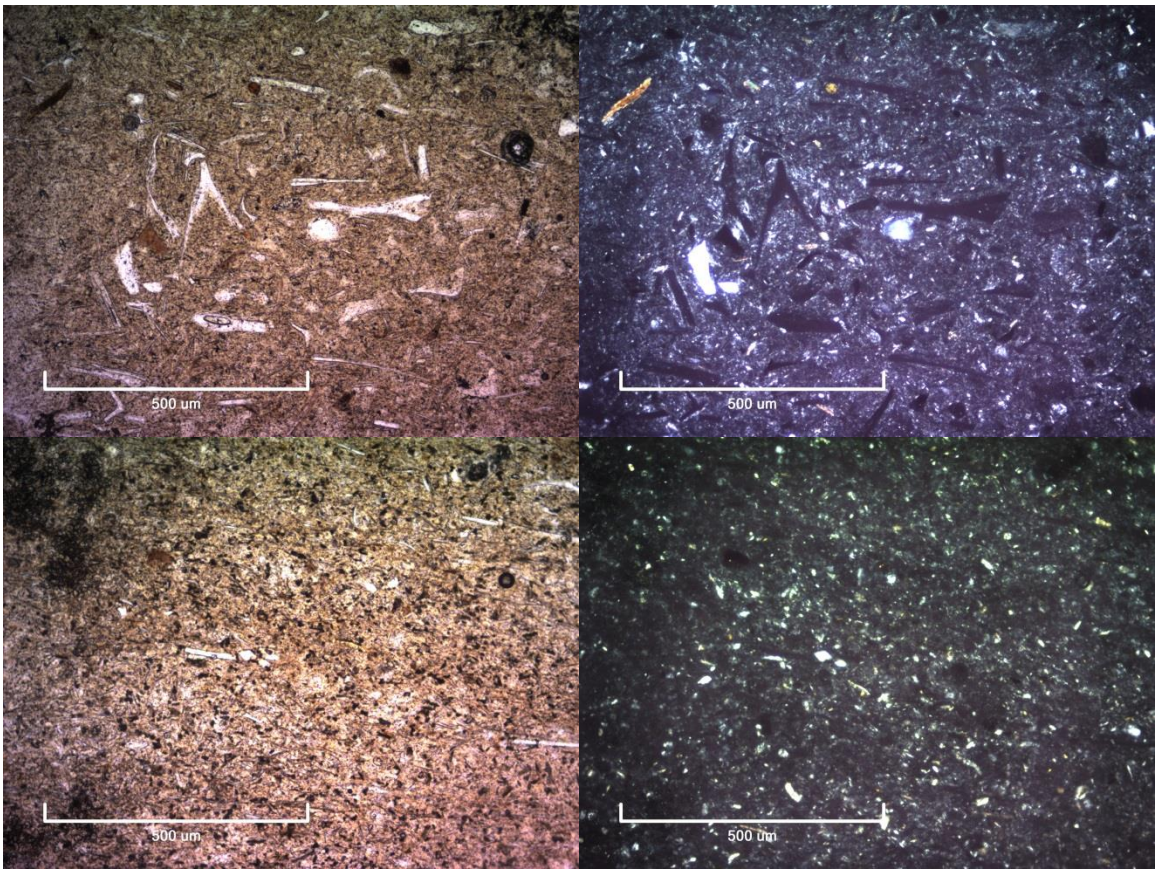
500 um
500 um
500 um
500 um

LB11

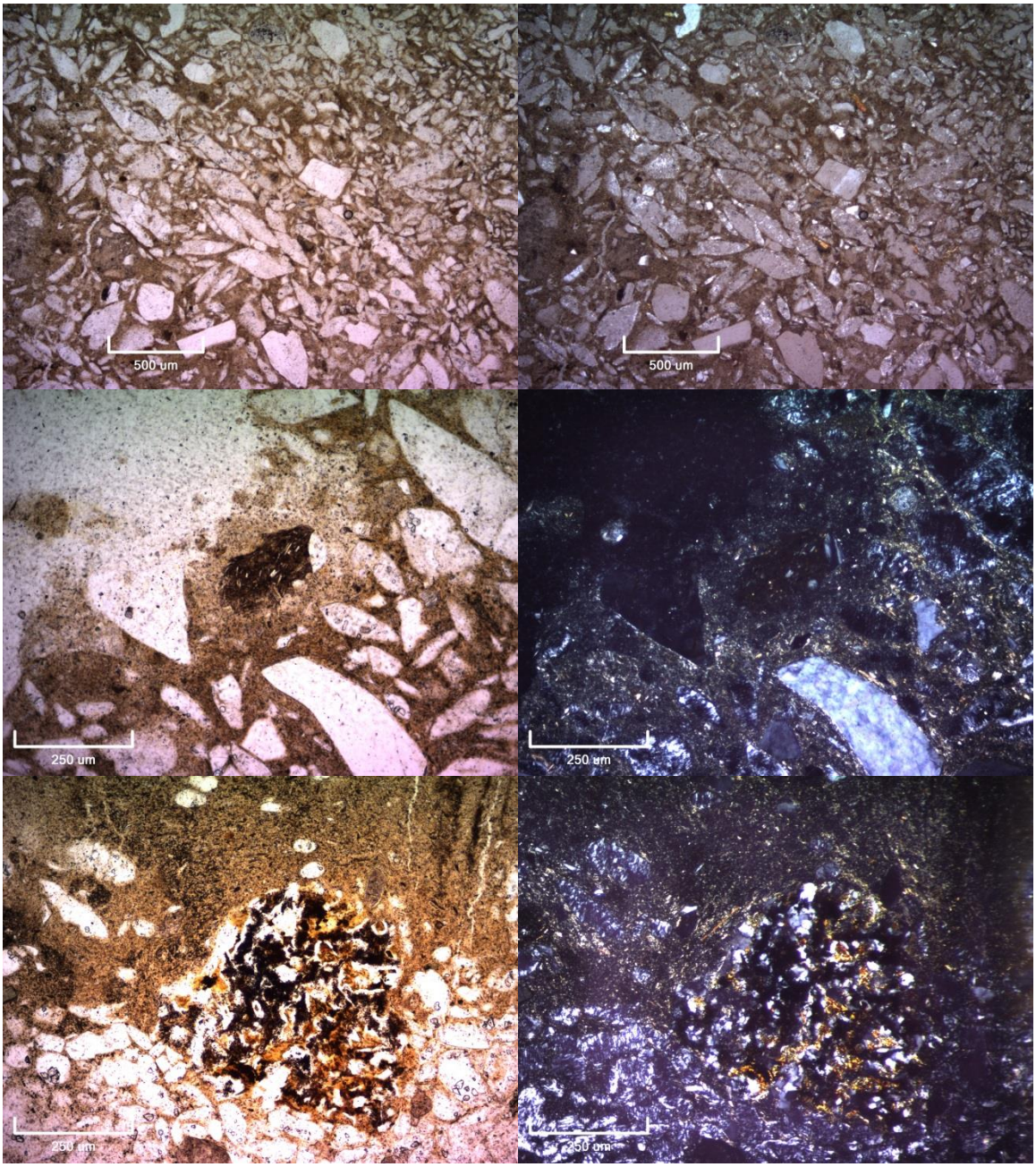

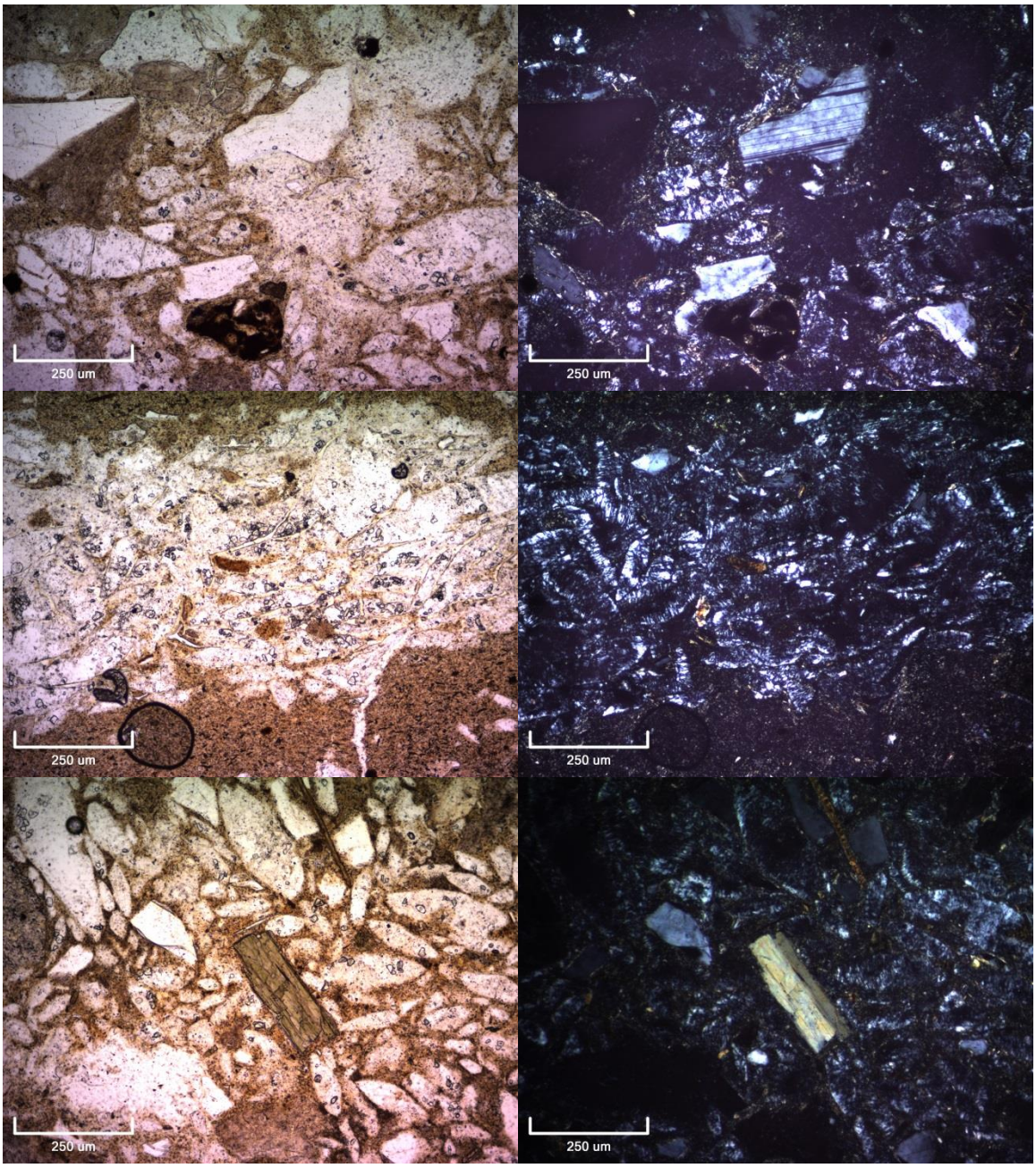
250 um
250 um
250 um
250 um
250 um
250 um

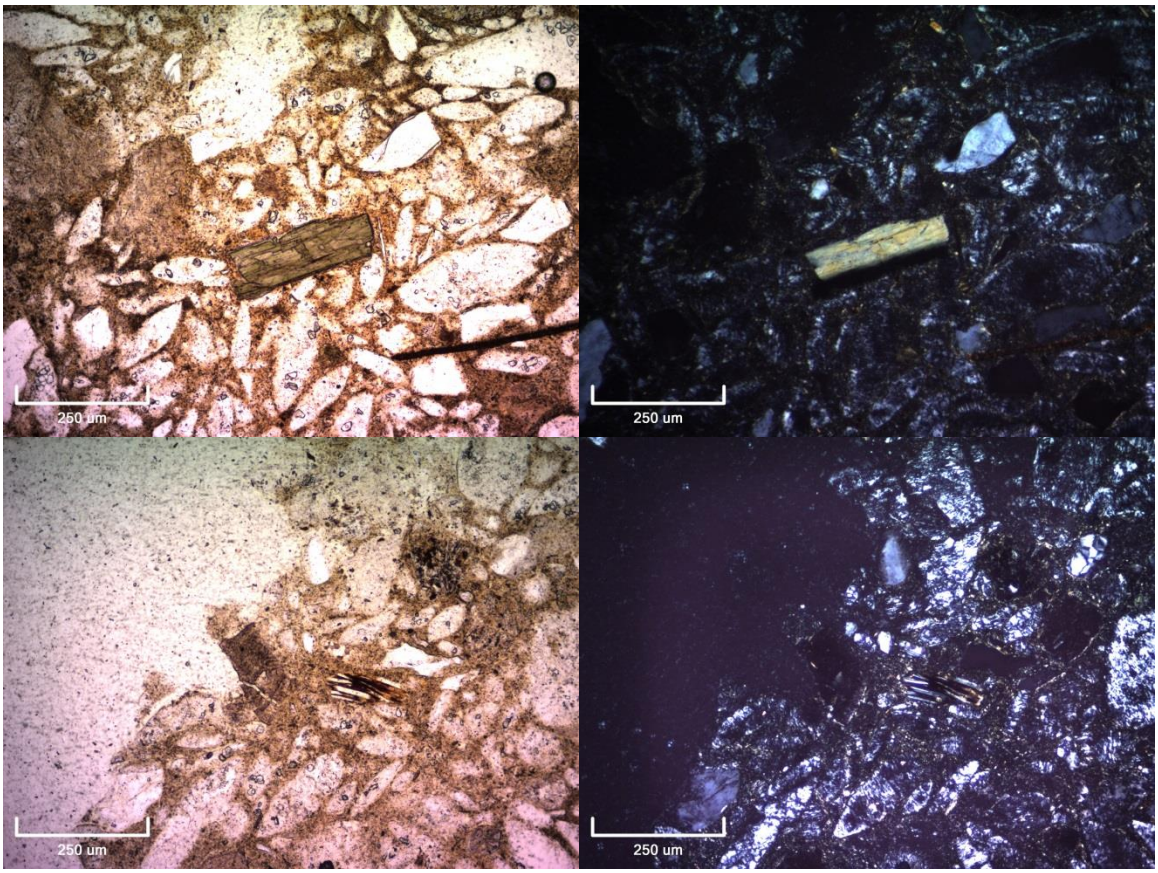
250 um
250 um
250 um
250 um

LB13

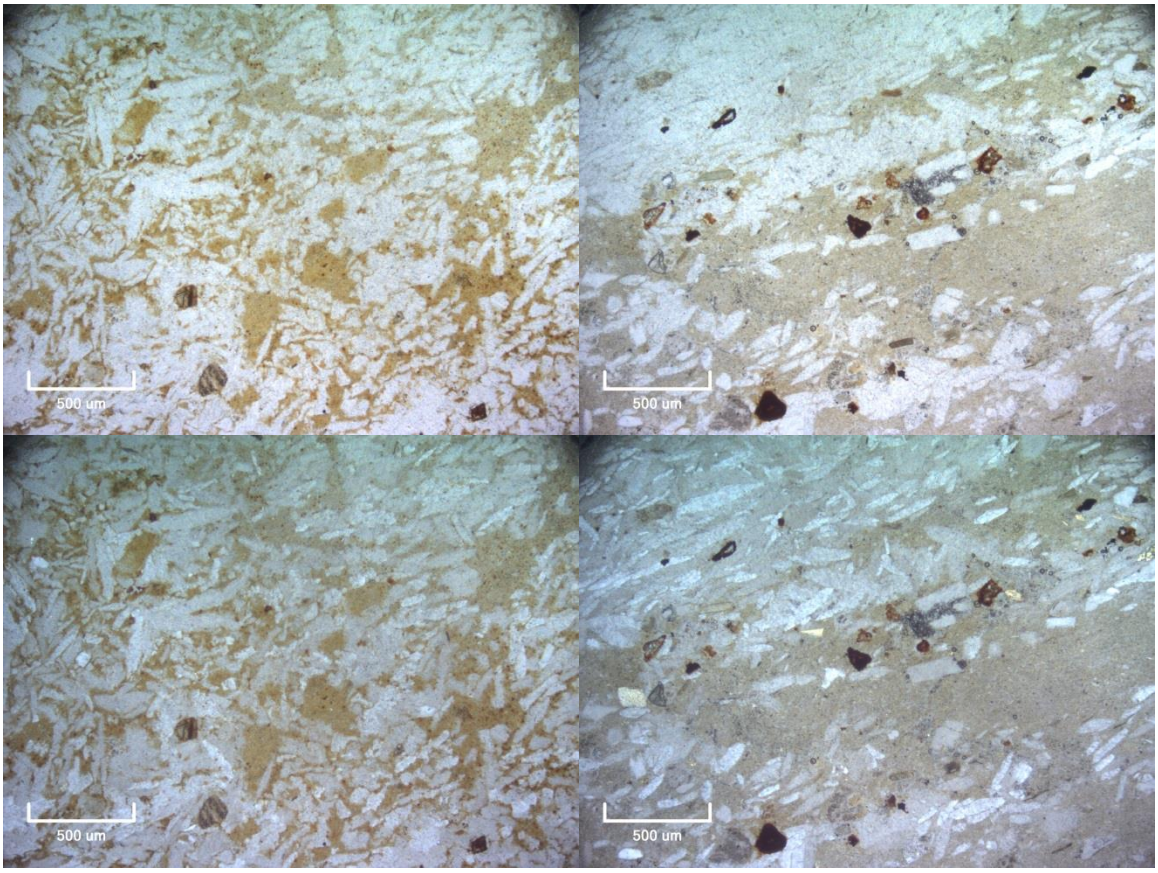

LB18

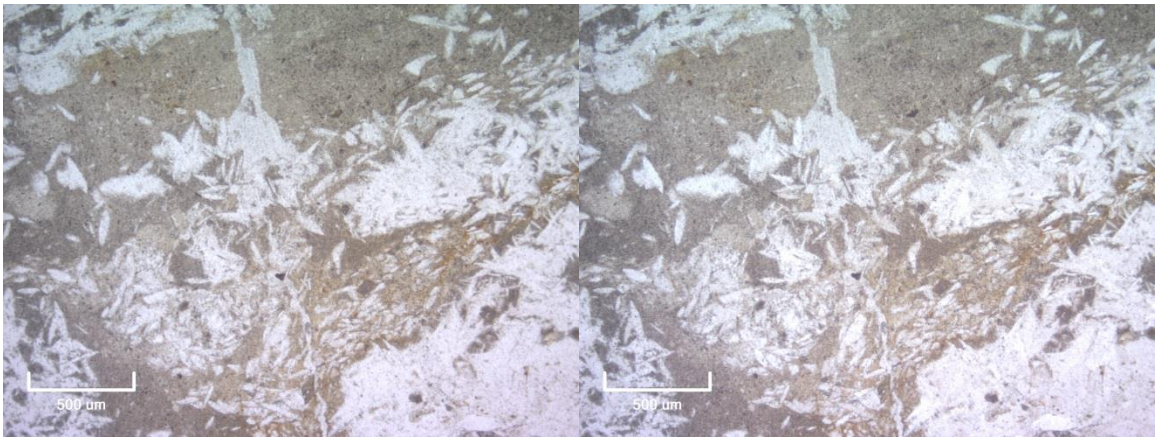

LB20

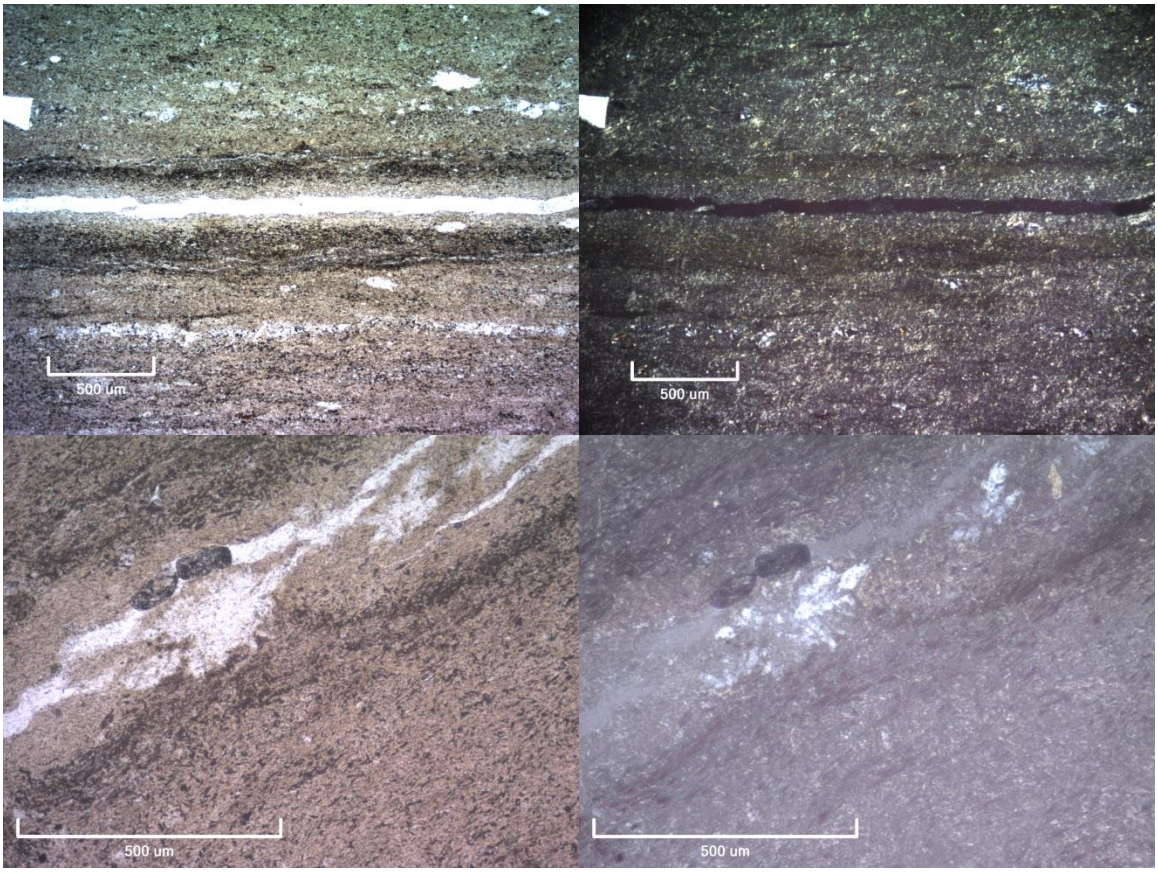

LB21

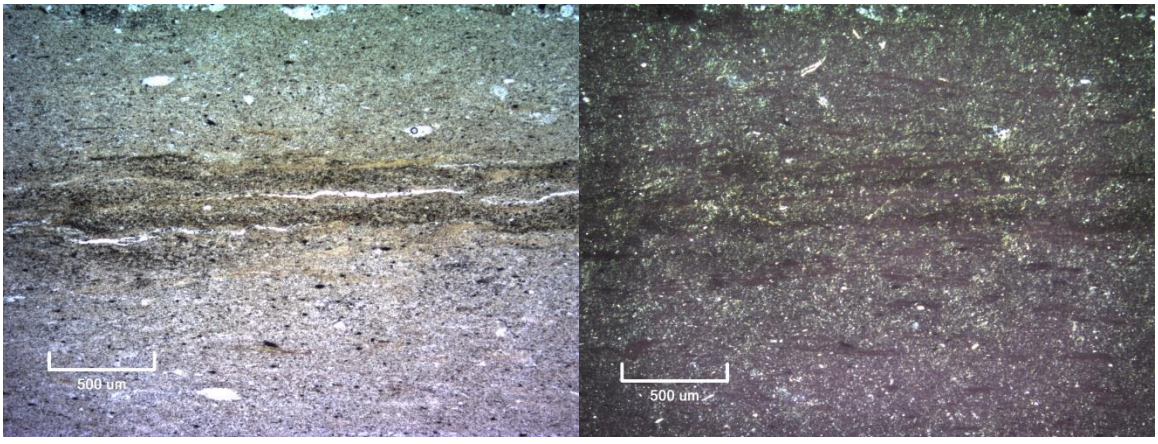

LB26

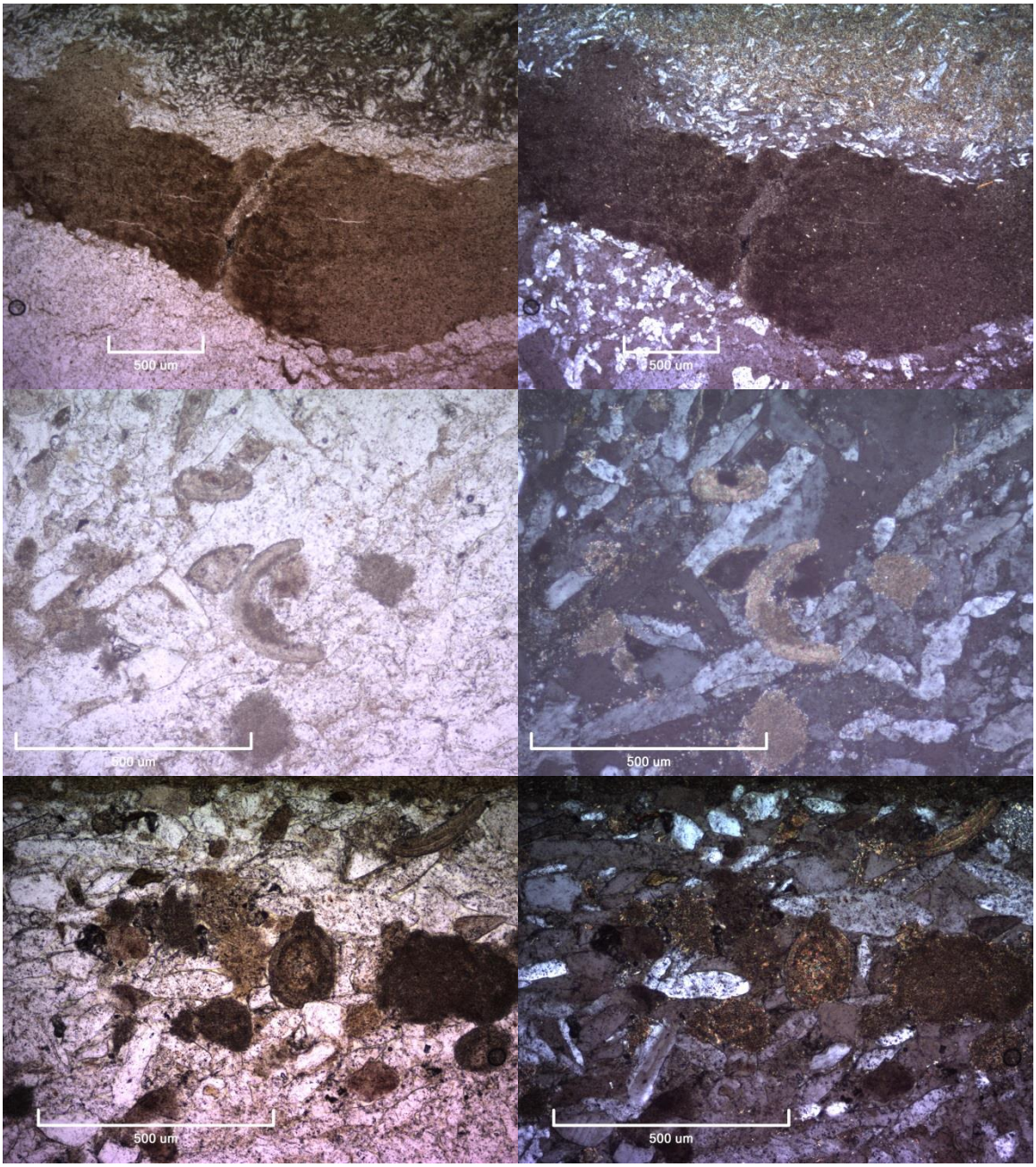

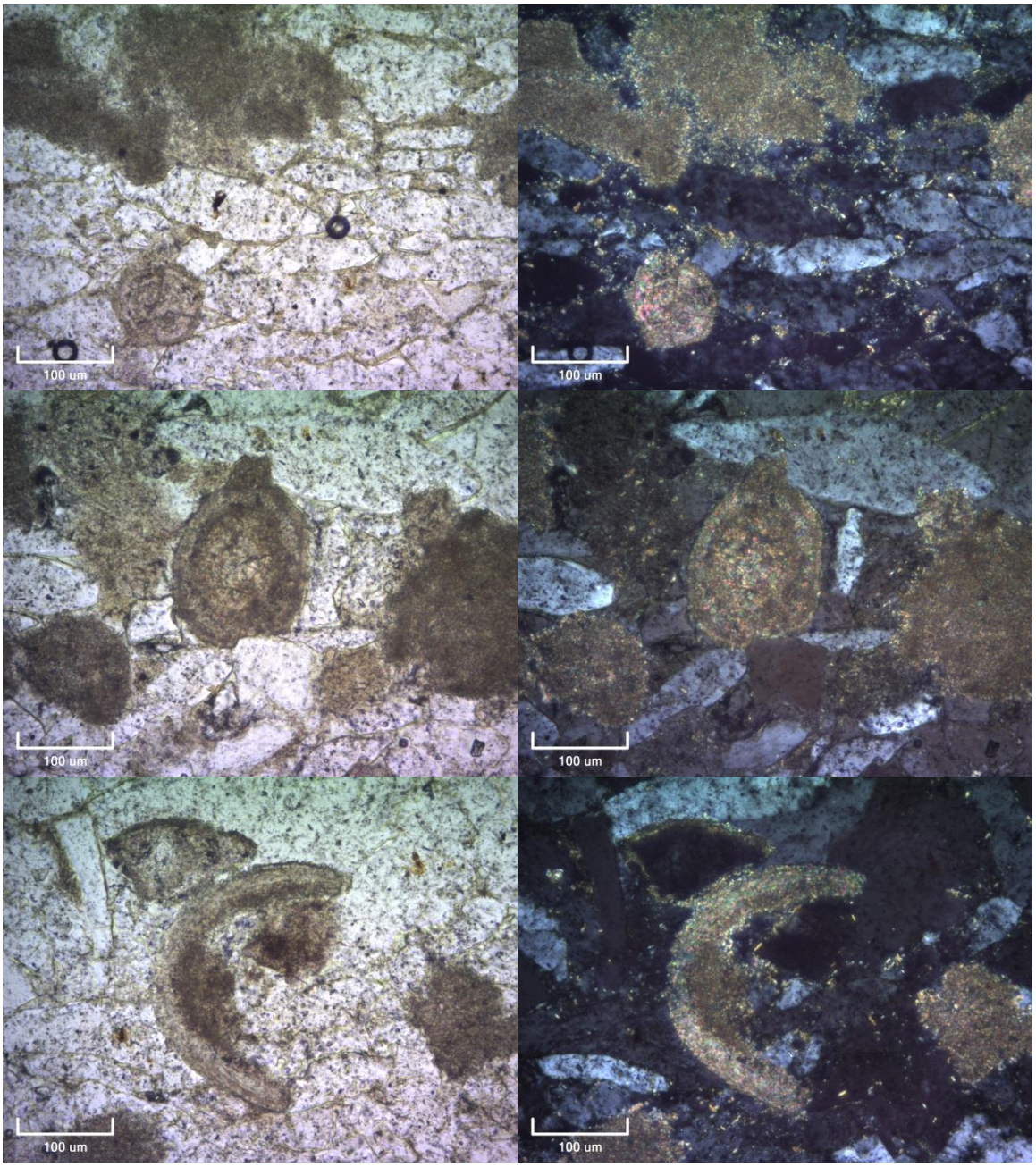
100 um
100 um
100 um
100 um
100 um
100 um

LB30

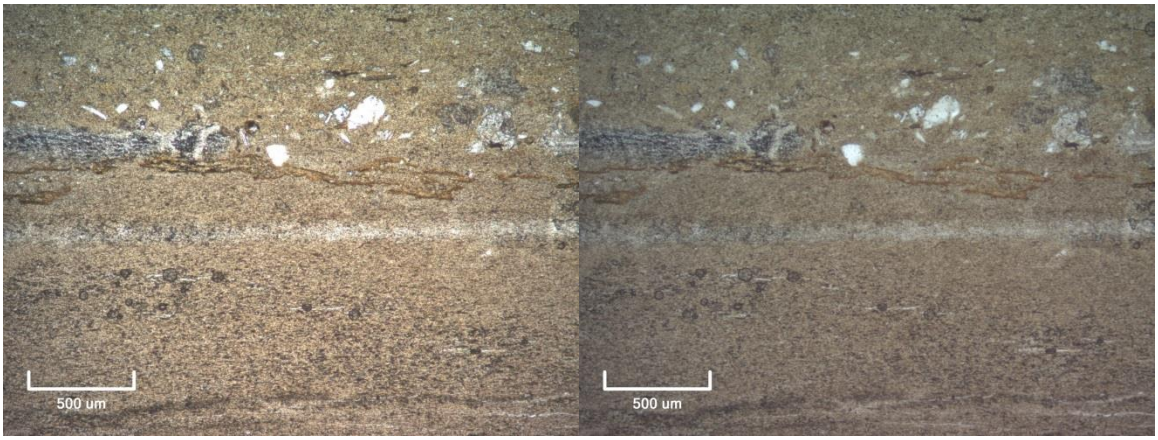

LB31

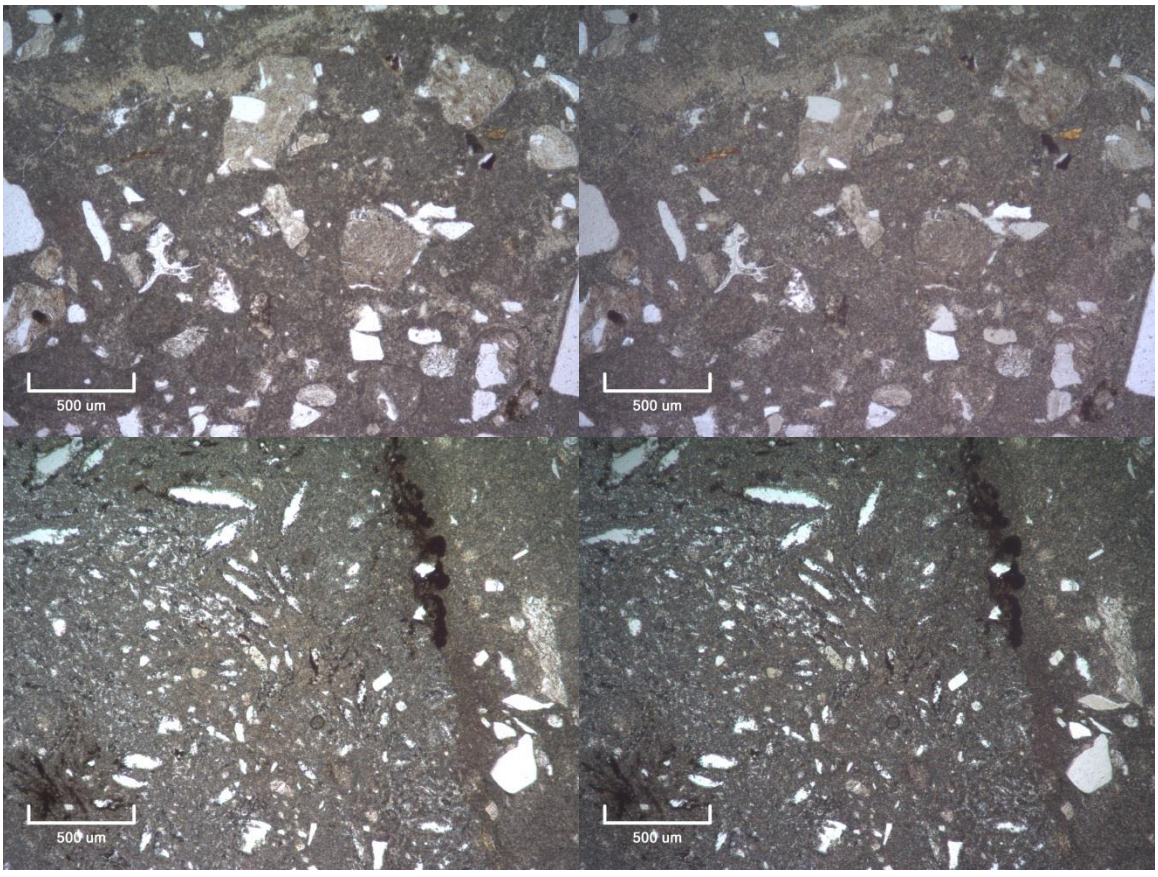

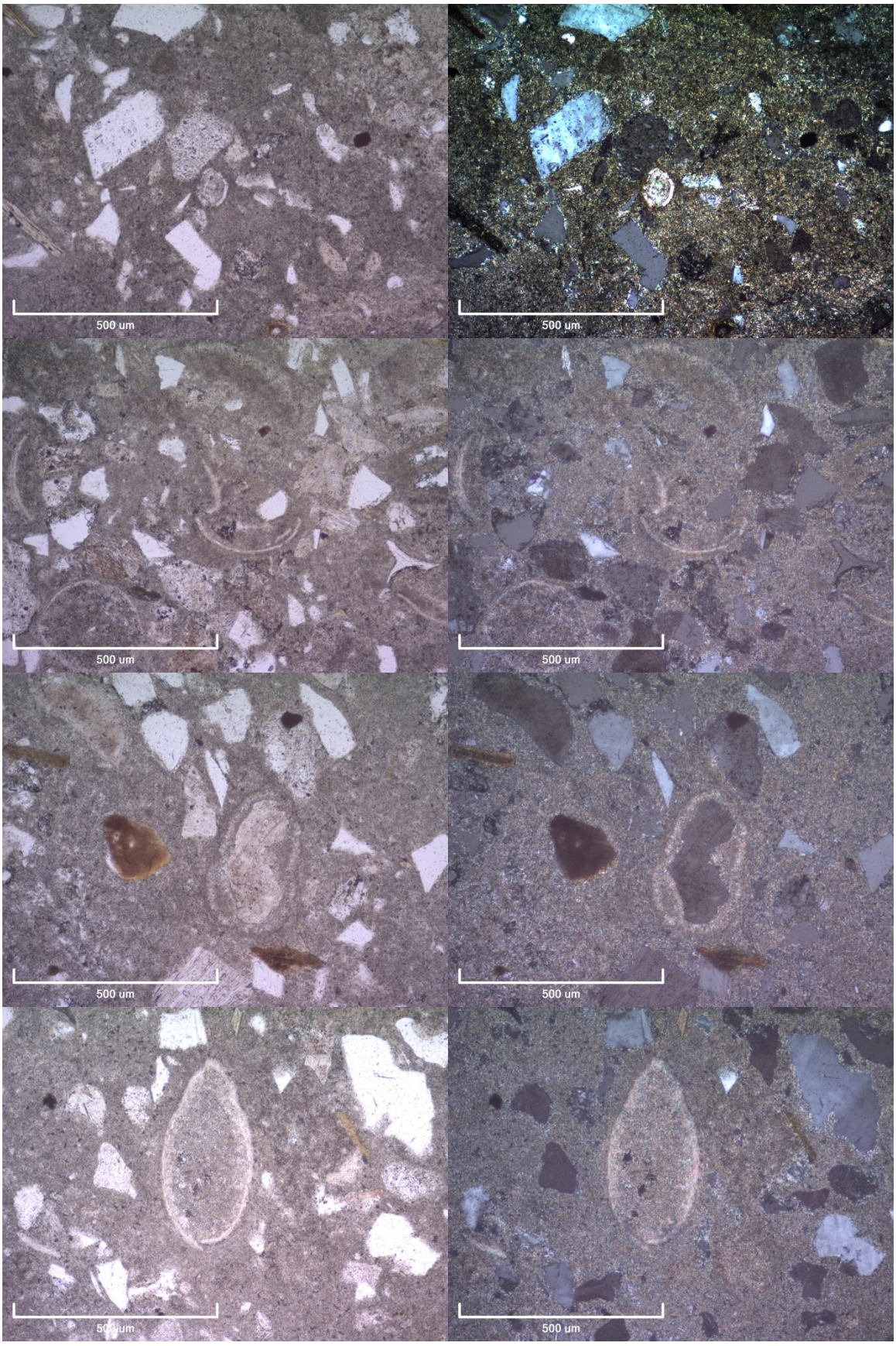
500 um
500 um
500 um
500 um
500 um
500 um
500 um
500 um

LB34

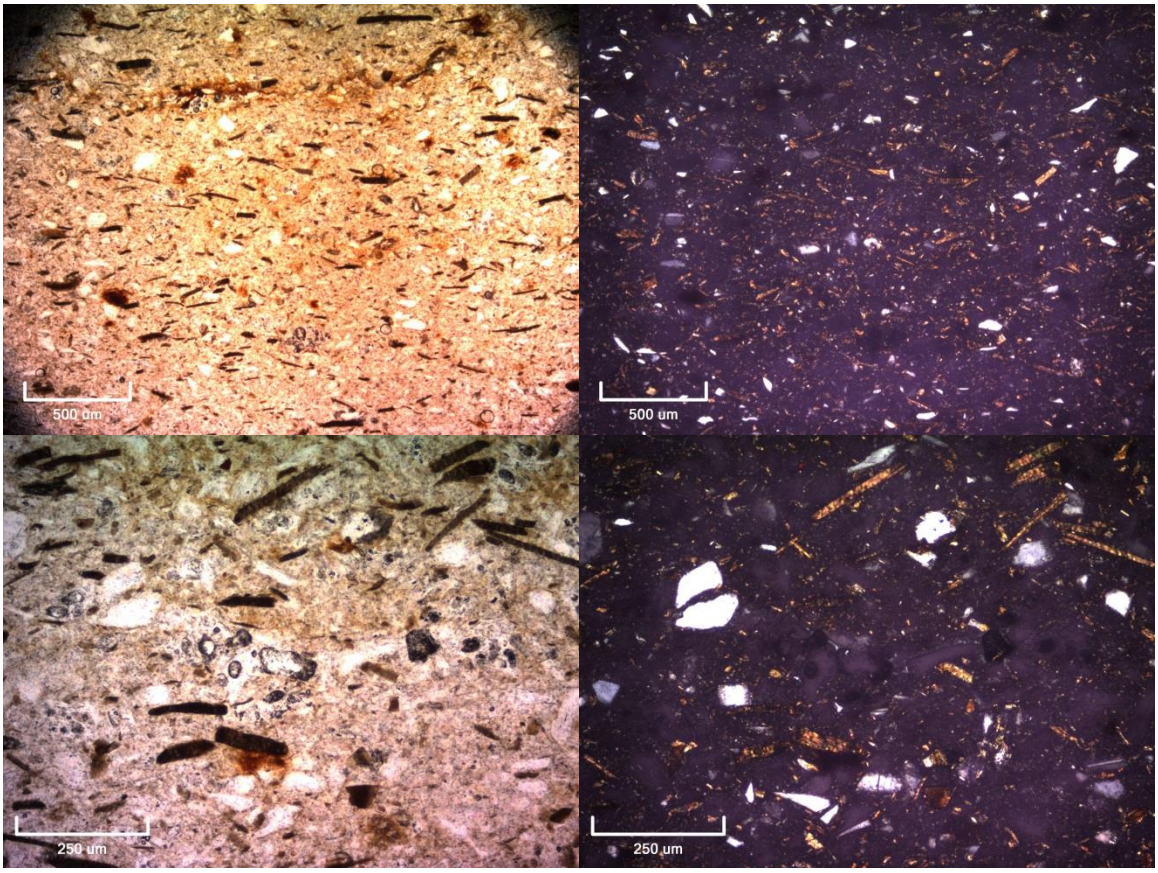

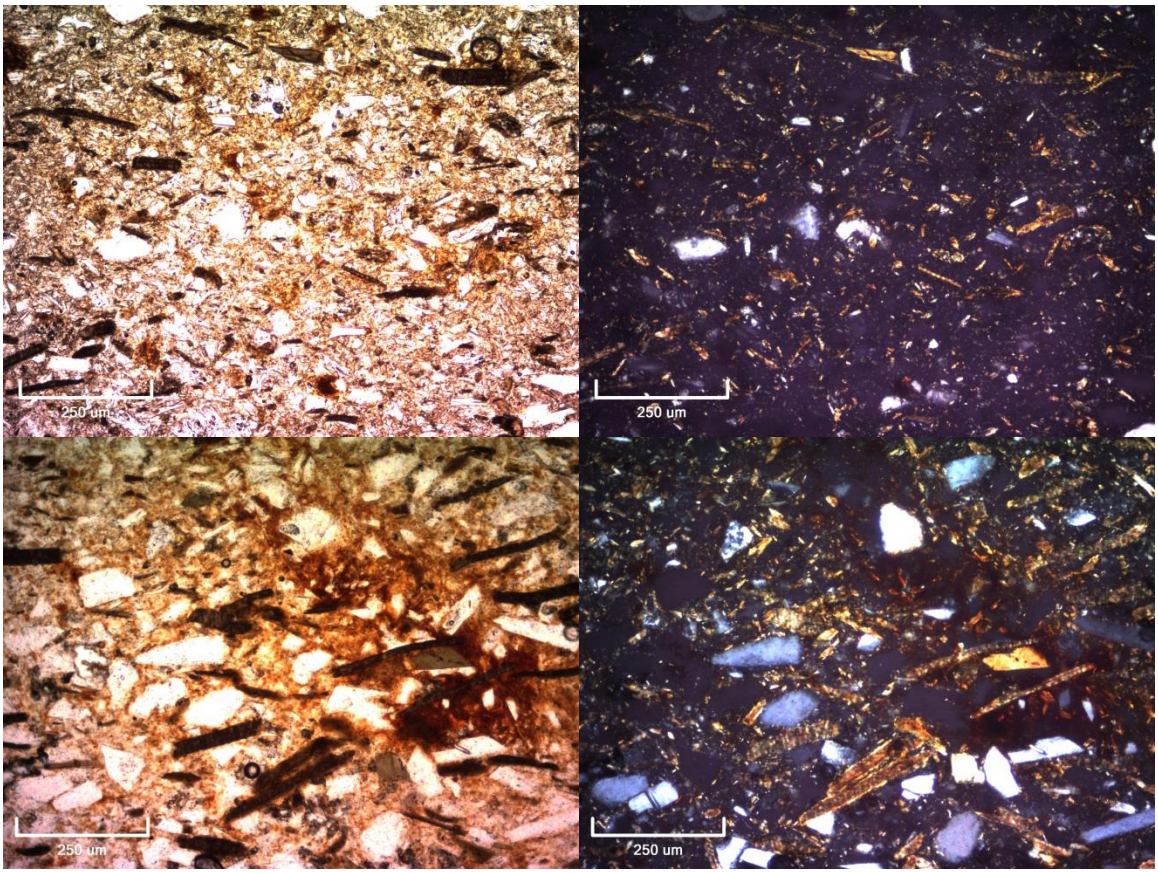
250 um
250 um
250 um
250 um

LB35

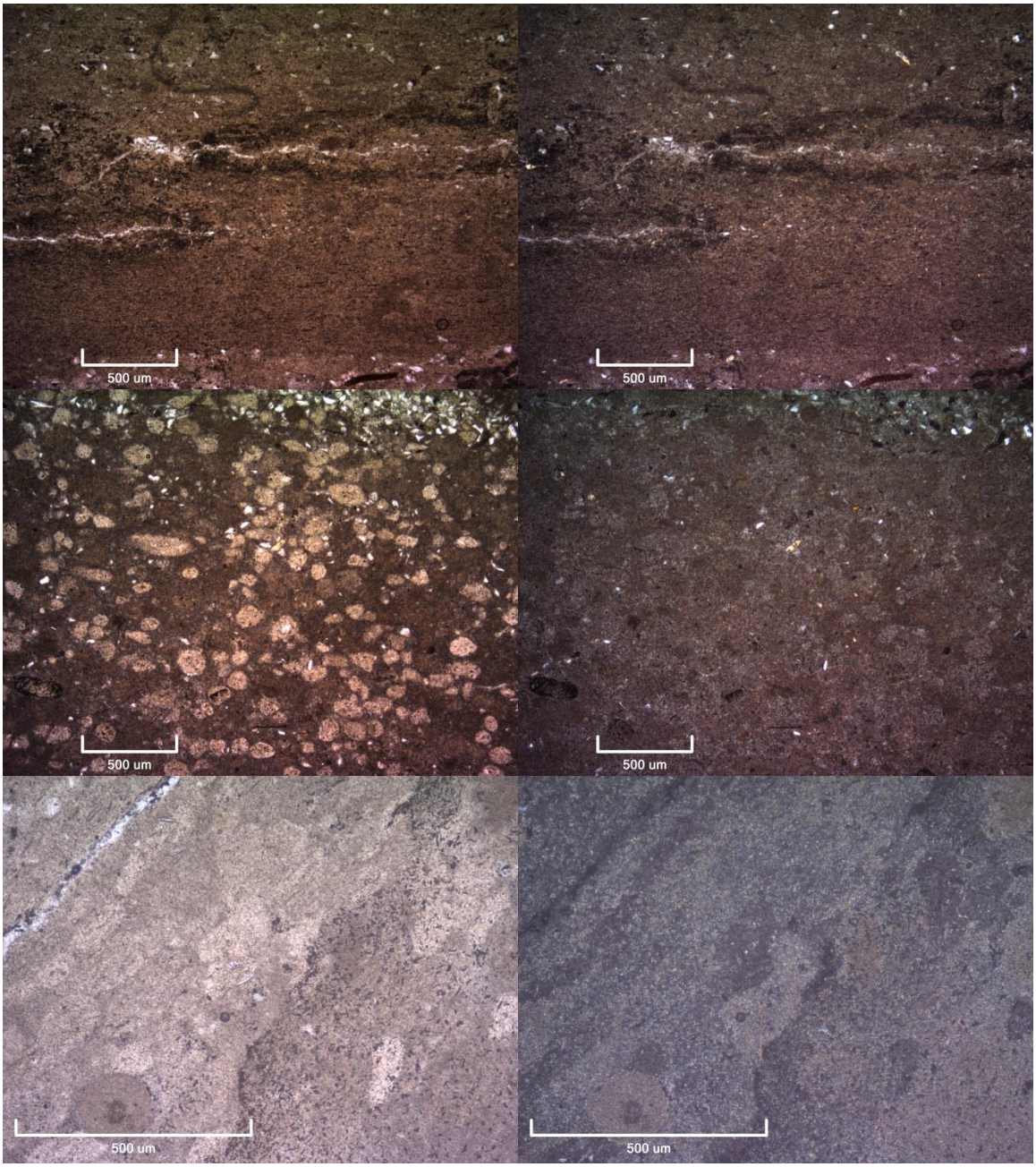

LB40